Vietnam Journal of Marine Science and Technology 2022, 22(4) 337–362

Vietnam Academy of Science and Technology

Vietnam Journal of Marine Science and Technology

journal homepage: vjs.ac.vn/index.php/jmst

The geochemical gas field in surface sediments in the Southwest sub-basin of East Vietnam Sea: distribution, origin, and comparative features with other regions of Western East Vietnam Sea

Le Duc Luong[1,2,*], Nguyen Hoang[1,2], Anatoly Obzhirov[3], Ryuichi Shinjo[4,5], Renat B. Shakirov[3]

[1]*Institute of Geological Sciences, VAST, Vietnam*
[2]*Graduate University of Science and Technology, VAST, Vietnam*
[3]*V. I. Il'ichev Pacific Oceanological Institute, FEB RAS, Vladivostok, Russia*
[4]*Research Institute for Humanity and Nature, 457-4 Motoyama, Kamigamo, Kita-Ku, Kyoto 603-8047, Japan*
[5]*Department of Physics and Earth Sciences, University of the Ryukyus, Nishihara, Okinawa 903-0213, Japan*

Received: 7 July 2022; Accepted: 21 August 2022

ABSTRACT

We analyzed 39 gas samples, including carbon dioxide, hydrocarbon gases C1–C4, hydrogen, and helium, in surface sediment from 19 gravity cores collected from the SW sub-basin of the East Vietnam Sea (EVS) using the headspace and vacuum degassing methods. Based on the result, we discussed the distribution and origin of gases in the southwest sub-basin EVS surface sediments. The sediments are mostly clay and silty clay containing methane ranging from 0.5–440 ppm. The anomalous concentrations of methane, helium, and hydrogen occur along the continental slope in the Nam Con Son basin of Southwest EVS. Methane is the dominant gas compared to other detected hydrocarbon gases, including ethylene, propane, and butane. Based on comparative results, the background methane concentrations in surface sediments decrease from South to North, from the southwestern sub-basin of the East Vietnam Sea to the Phu Khanh and the Red river basins. We propose the presence of a large-scale degassing zone of hydrocarbon gases and discuss the gases' origin in surface sediments based on hydrocarbon gas ratios, carbon isotope compositions of carbon dioxide and methane, and the relationship between geochemical characteristics of surface sediments and fault system, and surface sediment gases.

Keywords: East Vietnam Sea, hydrocarbon, methane, background concentrations.

[*]Corresponding author at: Institute of Geological Sciences, 84 Chua Lang, Dong Da, Hanoi, Vietnam. *E-mail addresses:* leducluong@igsvn.vast.vn

https://doi.org/10.15625/1859-3097/17398
ISSN 1859-3097; e-ISSN 2815-5904/

INTRODUCTION

The East Vietnam Sea (EVS) is situated at the junction of the Eurasian, Pacific, and Indo-Australian plates and is an immense marginal sea in the Western Pacific [1]. Many scientists have paid attention to the EVS during several recent decades because of its formation, evolution history, crucial geopolitical position, and oil potential. The main interest is EVS's geology, geophysics, oceanography, and gas-geochemical fields [2–7]. Some studies focus on methane distribution in the seawater (e.g., Tseng et al., (2017); Luong et al., (2019) [2, 6]), methane flux in the water-atmosphere interface (e.g., Shakirov et al., (2018); Shakirov et al., (2019) [4, 5]), or methane distribution in sediments from the Northern and Southwestern areas of EVS (Zhang et al., (2018), Luong et al., (2021) [3, 7]). However, there is no detailed study of gas distribution in sediment at a large scale in western EVS. According to Shakirov et al., (2017) [8], the EVS belongs to the Eastern Asia gas hydrate belt, including the Bering Sea, the Sea of Okhotsk, the Sea of Japan, the East China Sea, the EVS, and Southward to off-shore New Zealand.

Shakirov et al., (2018, 2019) [4, 5] reported five zones of methane emission along the route of the R/V "Akademik Boris Petrov" 2017 expedition, from the Taiwan Strait to the shelf of Malacca Peninsula based on analytical results of methane flux into the atmosphere in the EVS. Noticeably, the fourth zone, located on the eastern side of the Nam Con Son basin, has the most intensive values of methane flux and indicates the region's high oil and gas prospects. In addition, low methane concentrations were found in the deep-water (500–3,800 m), while higher methane concentrations were observed in the shallower water (30–500 m) in the EVS [6]. This contrast variability of dissolved methane concentrations in the bottom water may coincide with the methane distribution in surface sediments of the sea.

The Cruise 88 of the R/V "Akademik M.A. Lavrentyev" was conducted in November 2019 in three regions in the Western EVS [9], comprising the Southwestern part of the EVS in the Nam Con Son area, the area of Phu Khanh basin in the Central Vietnamese shelf, and the area of the Red river sediment basin (Fig. 1). Many essential data on geology, geophysics, and oceanography obtained from this cruise provide new insights into the Vietnamese continental shelf and the adjacent deep-sea basins [9]. Besides, data on gases in sediments from the southwestern sub-basin was also obtained during the D/K 105 in August–September, 2019 [7]. This study aims to elucidate the distribution and origin of gas fields in surface sediments in the Southwest sub-basin of EVS, the presence of a large-scale degassing zone of hydrocarbon gases, and comparative features of the study with other regions of western EVS.

GEOLOGICAL SETTINGS

The EVS is located at the intersection of the Eurasian, Pacific, and Australian-Indian plates [1]. The process of opening the EVS occurred during the Cenozoic period according to the continental extrusion mechanism leading to the oceanic crust extension. Following the studies of Taylor and Hayes (1980, 1983); Briais et al., (1993); and Li et al., (2015) [1, 10–12], the opening of the EVS started and ended between 32 and 16 million years ago (Oligocene - Miocene). Basaltic volcanism occurred widely during and after the oceanic crust spreading, which continues to this day. The IODP 349 drill hole U1433, located in the deep Southwest EVS basin, recorded layers of lavas hundreds of meters thick [1].

Fault systems are an essential condition in the formation and movement of gases in the sediments, forming various-scale degassing zone. In recent decades, many geological and geophysical studies have been conducted in the southwestern regions of the EVS for oil and gas exploration [13]. Many studies (e.g., Li et al., (2013); Ding et al., (2016); Phach et al., (2018)) [14–16] have focused on sedimentary, tectonic, and magmatic processes in the Southwestern sub-basin EVS. Our study area includes a part of the Southwest sub-basin of deep water EVS and the Eastern part of the

Nam Con Son basin. In the Southwest sub-basin, an old spreading axis extended 400 km Southwestward from 23.6 to 16 million years ago [1, 14, 15]. According to PetroVietnam (2005) [13], two fault systems in the Nam Con Son basin area are the North-South fault system distributed in the Western part and the Northeast-Southwest fault system that originated from the center of the basin and developed Eastward. The Eastern part of the Nam Con Son basin is cut by the 109^o meridian fault system, which is a fault zone stretching nearly 1,000 km on the continental shelf of Central and South-Central Vietnam [17].

Liu et al., (2016) [18] pointed out that the Indochina peninsula contributes a large amount of sediment to the EVS, mainly from the Red river in the North and the Mekong river in the South. In particular, the sediment discharge from the Mekong river into the Southern part of the EVS is estimated at 160 million tons/year [18, 19]. Schimanski and Stattegger (2005) [20] evaluated the Holocene sedimentation rate along the Vietnamese continental shelf and showed that the Southern shelf has a low sedimentation rate, about 5–10 cm/1,000 years. Wang and Li (2009) [21] noted that the surface sediments in the studied area mainly consisted of terrigenous sand and silty sand in shallow water and clay silt in deep water.

MATERIAL AND METHOD

Surface sediment and gas samples were collected from the gravity cores during two expeditions in the EVS, one was the DK105 in August–September, 2019, and the other was the R/V Akademik M.A Lavrentyev ship in November 2019 (Figure 1). These cruises belong to Vietnam National Research Program KC09/16–20 and the project "First joint expedition on marine geophysics, geology and oceanography between VAST and FEBRAS by R/V Akademik M.A. Lavrentyev in the South China Sea" QTRU.02.05/19–20.

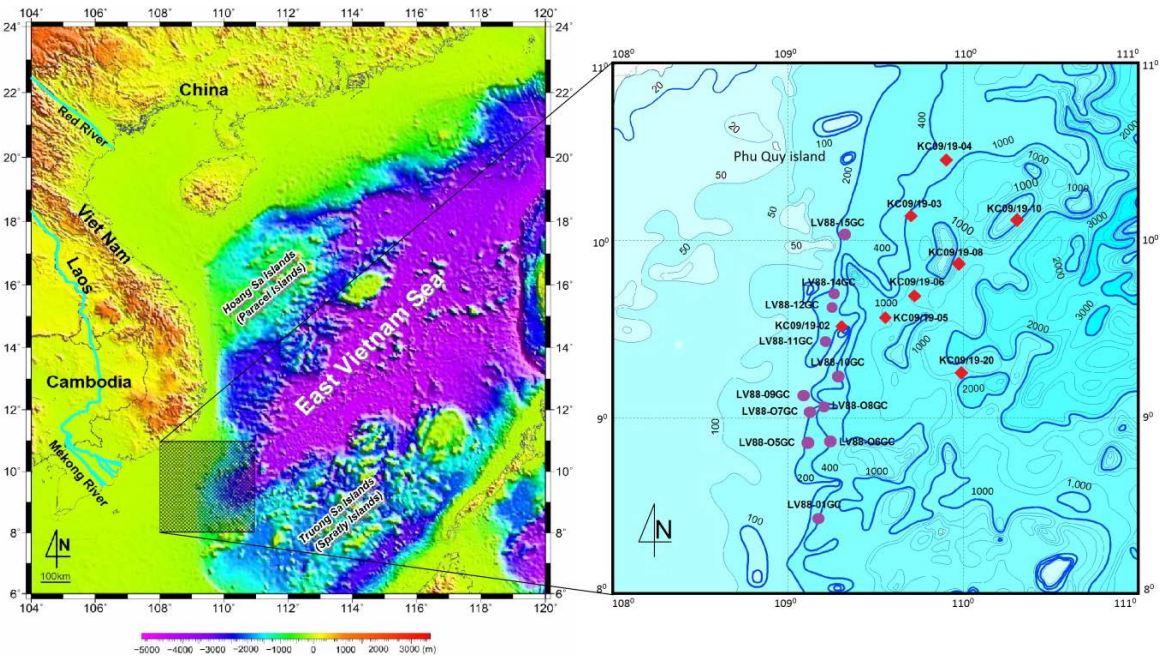

Figure 1. Location map of the Southwestern sub-basin EVS and gas sampling locations in surface sediments. The purple circle and the red diamond are, respectively, the sampling locations of the R/V Akademik M.A Lavrentyev and DK105 in 2019

Sediment samples taken from PVC pipes immediately after pulling up of gravity cores were contained in plastic bags and fully recorded with labels and depths of the core, then stored in a refrigerator to preserve their physical and chemical properties. The grain-size analysis of sediment samples was conducted using a Horiba LA-960 (Laser scattering particle size distribution analyzer) at the Institute of Geological Sciences, Vietnam Academy of Science and Technology. Trace and major element compositions of the sediment samples were processed and studied at the University of the Ryukyus, Okinawa's geochemistry laboratories, following procedures described in Luong et al., (2021) and Hoang et al., (2021) [22, 23]. The total organic carbon concentration, the total sulfide, and nitrogen were analyzed respectively by the Walkley Black method (TCVN 9941:2011), the gravimetric (TCVN 9296:2012), and the Kjeldahl method (TCVN 6498:1999) at the National Institute of Agricultural Planning and Projection.

Figure 2. Gas sampling on board DK105 (top) and R/V Akademik M.A Lavrentyev (bottom)

The gas samples were taken on board the mentioned cruises, including 39 representatives from 19 gravity cores collected using the "head space" method (Figure 2). The gas samples were analyzed at the Laboratory of Gas Geochemistry of the POI FEB RAS using a Gas Chromatograph CrystalLux - 4000M, whereas helium and hydrogen were analyzed using a highly sensitive Portable Gas Chromatograph Gasochrome 2000. Sediment samples taken from the core using a 20 mL (or 60 mL) cut-off plastic syringe was placed in 20 mL glass vials filled with saturated saline and stored in a refrigerator until analysis in the onshore laboratory.

From the analytical results of gas samples, the statistical parameters of hydrocarbons, carbon dioxide, helium, and hydrogen were determined using SPSS software. Then, the threshold values, background concentration, and anomalies of the gases were calculated according to the boxplot method of Reimann et al., (2005) [24].

RESULT AND DISCUSSION

Surface sediment characteristics in the southwest sub-basin of East Vietnam Sea

Grain-size characteristics

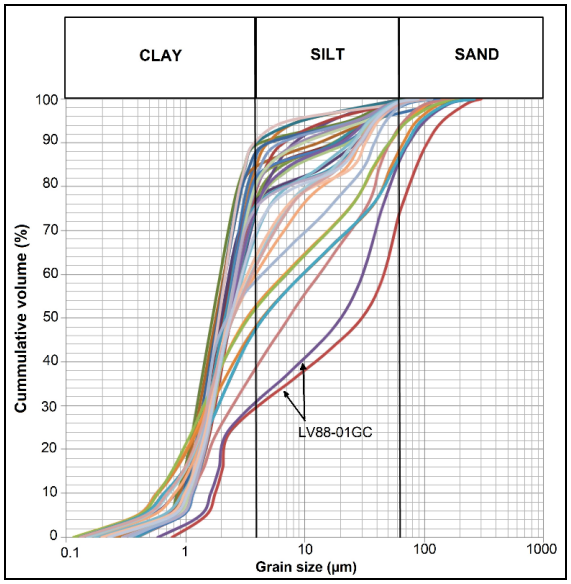

Figure 3. Grain-size cumulative curves of surface sediment samples (after Luong et al., (2021) [7])

Figure 3 shows the grain-size cumulative curves of 38 sediment samples from 19 gravity

cores. The most striking feature is the dominance of clay and silt compositions over the sand in those samples. Surface sediment samples in the area are predominantly clay, silty clay with clay concentration ranging from 37.53% to 96.37% (average 76.97%); silt content from 3.63% to 49.71%, an average of 18.10%; sand accounts for a small concentration, from 0 to 25.68 %, with an average of 2.25%. There are only a few samples with high sand concentration (more than 15%), mainly concentrated in the southwest of the studied area (samples LV88-01GC-1 and LV88-01GC-2). The remaining samples mostly have insignificant sand concentrations.

The results presented in Figure 3 show that the surface sediment samples are mostly clay and silty clay, while sand concentration is negligible. According to Folk (1974)'s classification [25], these sediments mostly fall into the mud field; a few remaining samples belong to the sandy mud category.

Geochemical characteristics of surface sediment

A set of 20 samples collected from 8 gravity cores in the studied area (Fig. 4) were processed to analyze major element and trace element compositions and organic chemical parameters.

The major element compositions of 20 sediment samples show that the SiO_2, Al_2O_3, CaO, and Fe_2O_3 are high compared to other oxides, with SiO_2 exhibiting the highest values among major elements, ranging from 32.58 wt.% to 52.15 wt.%; an average of 39.67 wt.%. Al_2O_3 and Fe_2O_3 concentrations range from 11.26 wt.% to 14.89 wt.% and 4.11–9.45 wt.%, respectively, while CaO concentration ranges from 3.10 wt.% to 13.93 wt.%.

Results of trace element compositions of 20 sediment samples, including Ag, As, Ba, Bi, Cd, Cs, Co, Cr, Cu, Mo, Ni, Pb, Sb, Sr, Zn, Sc, Y, and 15 elements of the lanthanide series (Le Duc Luong, unpublished data).

The rare earth element concentrations are normalized to a chondrite value (after Anders and Grevesse (1989)) [26], showing a gradual decrease from light to heavy rare earth elements, with a strong negative Eu anomaly observed for all samples (Fig. 5). The trace element contents are also normalized to an upper continental crust composition (UCC) [27, 28] for comparison (Fig. 5). A similar distribution pattern is also observed for the upper continental crust (UCC) and in sediments of modern plains [27, 28], suggesting that the surface sediments in the studied area have a continental provenance.

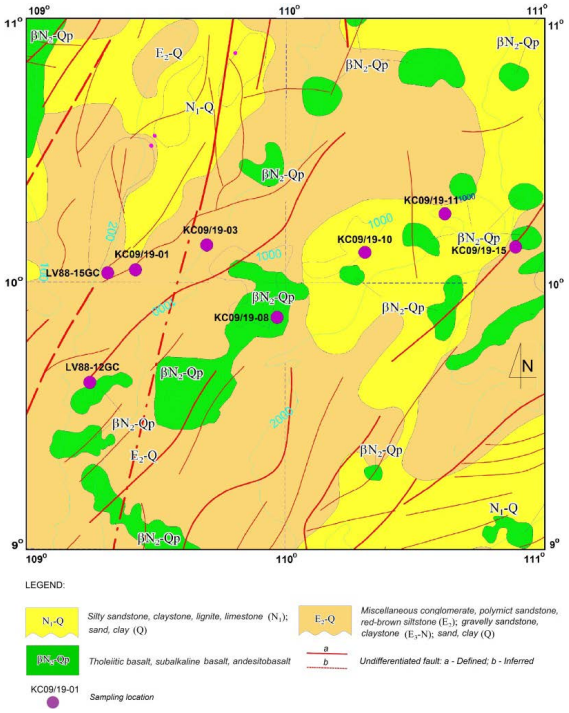

Figure 4. Location of surface sediments taken from gravity cores for geochemical analysis (after Geological map, geological resources of Vietnam and adjacent sea regions, scale 1:1.000.000 [29])

The organic chemical parameters of 20 surface sediment samples were analyzed, including total organic carbon (TOC), sulfide, and nitrogen. The analytical results showed that the total organic carbon concentration in the samples varies from 0.18% to 1.45%, with an average of 0.83%. Total organic carbon concentration represents different values between different sampling sites and also within the sediment cores. Sediments from

deeper water depths often have lower TOC values than shallower water depths, reflecting father distances from organic matter supplies. In addition, the organic matter will be more influenced by the oxidation process during the deposition in the deeper water depth [30]. The total sulfur concentration in the samples ranged from 0.137% to 2.339%; samples LV88-12GC-1 and LV88-12GC-2 show significantly higher than the others. In contrast, the total nitrogen concentration in the samples is the lowest among the gases analyzed, ranging from 0.067% to 0.106%.

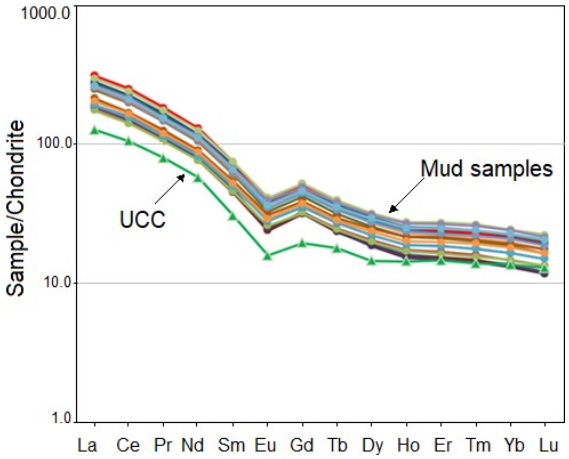

Figure 5. Chondrite-normalized rare earth element patterns of surface sediment samples

Distribution of gases in surface sediments in the SW sub-basin of East Vietnam Sea

Distribution of hydrocarbon gases in surface sediment of the SW sub-basin of East Vietnam Sea

The hydrocarbon gas concentrations in the surface sediments from 19 gravity cores in the southwest sub-basin are presented in Table 1. The concentrations of hydrocarbon gases significantly differ between the shallow water areas on the continental shelf and slope-and-deep water areas. The difference reflects the similarity with the distribution of methane concentration in the bottom water layer of the western EVS, whereby the methane concentration in the bottom water of the deep-water area is significantly smaller than in shallow-water regions on the continental shelf and slopes [6]. The concentrations of hydrocarbons and carbon dioxide in surface sediments collected at the continental shelf and slopes (mainly by the Lavrentyev cruise) are much higher than those in the deep-water areas (managed by the DK105 cruise).

For the entire studied area, the methane concentration in the surface sediments, ranging from 0.5 ppm to 440 ppm (Table 1, Fig. 6), was detected in all the analyzed samples. Figure 6, showing the highest methane distribution area, reveals the difference in the methane concentration between the shallow water area on the continental shelf and slope and the deep-water sub-basin EVS. Thus, the methane concentration in the surface sediments decreased markedly from West to East with increasing water column depth (Fig. 6). In shallow water areas, methane concentrations tend to be higher in the central region and decrease in Southward and Northward directions. Besides, Figure 6 also shows the methane concentrations in each core according to the sampling intervals. The highest methane concentrations are at stations LV88-07GC, LV88-08GC, LV88-09GC, and LV88-10GC, managed by the Lavrentyev expedition.

The other hydrocarbon gases heavier than methane, such as ethylene, ethane, propane, i-butane, and butane in the sediments, were also determined for concentrations (Table 1). The most noticeable feature is the predominance of methane gas concentration over other gases. Ethylene gas, ranging from 0 ppm to 70 ppm, was detected in 97.4% of the analyzed samples. Similarly, ethane was detected in 74.4% of sediment samples throughout the studied area and ranged from 0 ppm to 124 ppm. There is a marked difference in the higher values of ethane and ethylene gas in the surface sediments in the continental shelf and slope areas compared to the deep-water site; much like the case of methane, 87.2% of collected surface sediment samples contained propane gas, with concentrations ranging from 0 ppm to 50 ppm.

Meanwhile, butane in the sediment samples was presented with two isoforms, butane and

i-butane, found in 38.5% and 17.9% of the analyzed samples. In general, methane and other heavier gases have a similar distribution pattern, with a markedly higher concentration distributed in the shallow water areas of the continental shelf and slopes compared to the deep-water regions of the Southwest sub-basin EVS. The high values of hydrocarbon gas concentrations in surface sediments are mainly concentrated in the Central part of the shallow water area along the expedition of the Lavrentyev cruise.

Table 1. Concentrations of carbon dioxide and hydrocarbon gases in surface sediment of the Western EVS

Region	No.	Station	Depth (m)	Interval (cm)	CO_2 (%)	CH_4 (ppm)	C_2H_4 (ppm)	C_2H_6 (ppm)	C_3H_6 (ppm)	C_3H_8 (ppm)	i-C_4H_{10} (ppm)	C_4H_{10} (ppm)
I. The Southwest sub-basin East Vietnam Sea	1	KC09/19-02	754	20	0.11	1.4	0.08	0	0	0.04	0	0
	2			100	0.10	4.2	0.17	0.09	0	0.09	0	0
	3			200	0.13	3.2	0.13	0.02	0	0.04	0	0
	4	KC09/19-03	1113	20	0.10	3.7	0.20	0.02	0	0.03	0	0.01
	5			100	0.13	3.8	0.14	0.01	0	0.03	0	0
	6	KC09/19-04	640	20	0.12	2.3	0.11	0	0	0.03	0	0
	7			100	0.12	3.5	0.08	0	0	0.03	0.02	0
	8	KC09/19-05	754	20	0.09	2.9	0.13	0	0	0.04	0	0
	9			100	0.07	5.7	0.11	0	0	0.05	0	0
	10	KC09/19-06	1677	50	0.10	1.1	0.09	0	0	0.05	0	0
	11			100	0.14	1.1	0.09	0	0	0.03	0	0
	12	KC09/19-08	1985	20	0.08	0.7	0.06	0	0	0	0	0
	13			100	0.07	0.9	0.10	0	0	0	0	0
	14	KC09/19-10	1373	20	0.08	0.7	0.16	0.02	0	0.04	0	0
	15			100	0.14	1.3	0.13	0.01	0	0.03	0	0
	16	KC09/19-20	2123	20	0.13	0.5	0.13	0.01	0	0.03	0	0
	17			100	0.14	0.8	0.08	0	0	0	0	0
	18	LV88-01GC	400	20	1.59	98.3	11.07	34.87	0	10.55	0	1.67
	19			160	0.63	34.7	4.43	10.41	0	2.45	0	0.44
	20	LV88-05GC	243	20	1.12	146.1	7.87	59.28	0	19.38	0.35	3.77
	21			130	0.93	74.3	6.78	25.66	0	9.58	0.27	3.78
	22	LV88-06GC	852	330	0.56	60	10	20	0	0	0	0
	23	LV88-07GC	196	40	0.77	154	20	45	0	10	0	6
	24			100	2.40	400	64	124	0	24	0	8
	25	LV88-08GC	682	70	0.60	68	12	18	0	7	0	1
	26			260	1.67	256	56	56	0	14	0	0
	27	LV88-09GC	159	30	0.91	300	0	10	0	0	0	0
	28			70	0.70	57	6	20	0	50	0	1
	29	LV88-10GC	1011	40	1.95	79	11	18	0	4	0	1
	30			180	0.61	220	30	25	0	5	0	0
	31			310	1.57	440	70	65	0	24	0	0
	32	LV88-11GC	267	60	2.54	75.9	6.23	30.38	0	9.35	0	1.48
	33			260	2.24	66.4	4.67	17.38	0	5.43	0	0.94
	34	LV88-12GC	263	20	0.56	175.4	4.30	12.65	0	1.99	0	0
	35			70	0.27	27.3	2.50	3.58	0	1.06	0	0
	36	LV88-14GC	256	60	3.13	35.9	7.01	8.16	0	3.39	5.27	1.28
	37			210	1.54	42.5	9.32	8.83	0	2.94	4.96	0.84
	38	LV88-15GC	236	60	1.22	42.9	5.62	13.29	0	4.37	4.48	1.11
	39			210	1.86	47.1	6.30	7.20	0	2.08	3.45	0.49

Region	No.	Station	Depth (m)	Interval (cm)	CO_2 (%)	CH_4 (ppm)	C_2H_4 (ppm)	C_2H_6 (ppm)	C_3H_6 (ppm)	C_3H_8 (ppm)	i-C_4H_{10} (ppm)	C_4H_{10} (ppm)
II. Phu Khanh basin	40	LV88-16GC	2300	80	4.77	55	14.00	16.00	0	8.00	0.50	2.70
	41			210	2.09	39	9.00	8.00	0	2.00	0	0.40
	42	LV88-17GC	76	20	1.20	164	24.00	70.00	0	20.00	0	0.00
	43			60	0.38	16	2.00	5.00	0	2.00	0	0.60
	44	LV88-18GC	380	40	1.99	35	7.00	10.00	0	5.00	0	1.10
	45			250	0.79	71	11.00	13.00	0	5.00	0	1.70
	46			340	0.58	33	4.00	4.00	0	1.00	0	0.20
	47	LV88-20GC	2400	160	0.70	32	4.00	9.00	0	3.00	0	0.60
	48			95	1.33	36	6.00	8.00	0	3.00	0	0.70
	49	LV88-21GC	139	20	0.91	33	5.00	11.00	0	4.00	0	0.90
	50	LV88-22GC	1240	40	0.37	20	2.00	2.00	0	1.00	0	0.50
	51	LV88-23GC	726	40	1.18	56	5.44	5.27	0	1.60	0	0
	52			140	1.63	107	10.12	10.01	0	2.84	0	0.65
	53	LV88-25GC	1905	30	2.18	125	18.37	29.27	0	11.46	0.57	2.37
	54			110	1.77	98	9.14	8.73	0	4.02	0.13	1.97
	55	LV88-28GC	705	60	1.60	48	5.05	6.13	0	1.48	0	0.18
	56			160	1.44	26	4.45	5.19	0	1.48	0	0.41
	57	LV88-29GC	336	270	1.07	32	5.08	5.52	0	1.67	0	0.47
	58			100	1.41	58	11.04	11.88	0	4.25	0	1.08
	59	LV88-30GC	195	60	1.16	51	7.24	8.40	2.69	2.69	0	0.65
	60			160	0.31	5	0.73	1.15	0	0.44	0	0.00
	61	LV88-32GC	1455	80	0.68	23	2.13	5.94	0	2.46	0	0.75
	62	LV88-35GC	1005	45	0.36	15	1.21	1.86	0	0.43	0	0
	63	LV88-36GC	759	130	1.86	196	12.37	21.86	0	6.02	0.18	0.91
	64	LV88-37GC	689	40	0.30	5	0.23	0.26	0	0.08	0	0.00
	65			95	0.24	4	0.10	0.15	0	0.00	0	0.00
	66	LV88-38GC	260	60	1.28	31	2.77	8.44	0	2.47	0	0.87
	67			160	0.68	14	1.45	3.09	1.18	1.18	0	0.43
	68	LV88-39GC	241	110	0.52	15	1.79	3.29	0	1.11	0	0.30
	69			210	0.22	3	0.11	0.13	0	0.05	0	0.00
	70	LV88-40GC	1039	60	0.70	16	2.43	4.19	0	1.19	0	0.74
	71			190	0.26	3	0.08	0.12	0	0.06	0	0
	72	LV88-41GC	798	240	0.30	11	0.86	2.25	0	0.72	0	0
	73	LV88-43GC	660	80	0.12	4	0.24	0.39	0	0.07	0	0
	74			210	0.10	2	0.04	0.04	0	0.05	0	0
	75	LV88-46GC	2283	80	1.157	49	10.03	16.46	0	6.28	0.22	1.26
	76			210	1.564	40	6.79	9.11	0	4.61	0.29	2.62
	77			340	0.190	2	0.08	0.11	0	0.10	0	0.00
	78	LV88-47GC	2139	90	1.402	39	6.76	7.45	0	1.76	0	0.37
	79			290	0.287	5	0.53	0.59	0	0.23	0	0
	80	LV88-48GC	874	90	3.10	79	4.42	14.05	0	4.01	0	1.23
	81	LV88-49GC	170	240	2.13	112	13.25	28.41	0	10.00	0.43	2.05
III. Red river basin	82	LV88-50GC	520	90	1.26	32	3.55	8.45	0	3.80	0.14	1.20
	83			240	0.97	28	4.97	5.70	0	2.75	0.10	1.35
	84	LV88-51GC	515	80	0.84	47	8.37	16.31	0	4.95	0.21	1.24
	85			210	1.18	33	5.31	7.51	0	3.15	0.08	1.07
	86	LV88-55GC	72	260	2.11	27	2.13	2.28	0	1.15	0	0.69
	87	LV88-56GC	62	70	0.37	11	1.10	1.12	0	0.41	0	0
	88			190	1.22	30	4.02	4.23	0	1.66	0	0.44

Note: Data of Region I from Luong et al., (2021) [7].

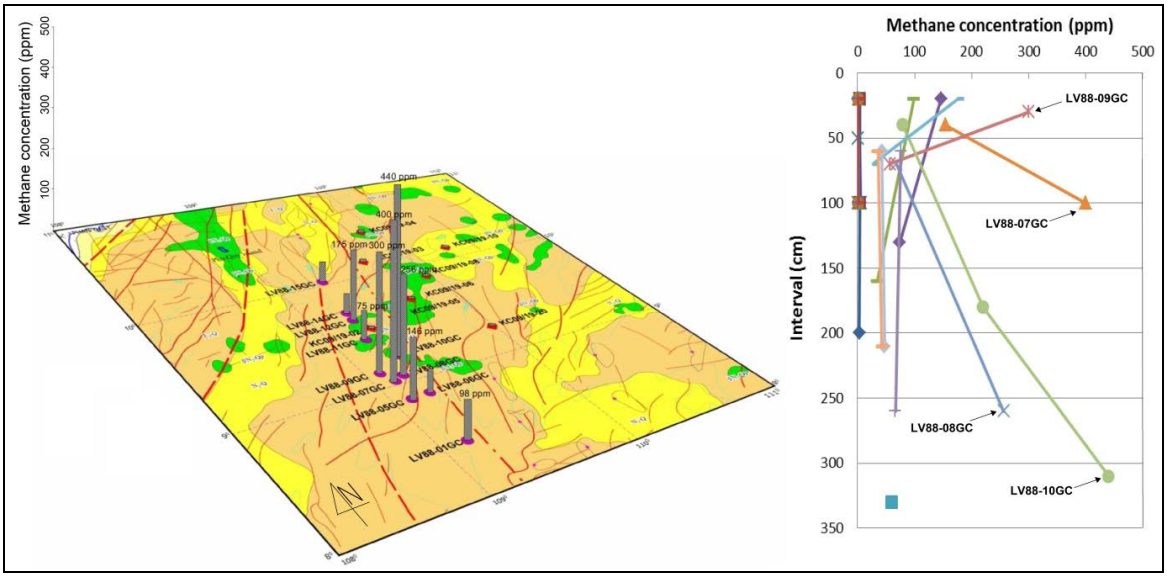

Figure 6. Distribution of methane concentration in surface sediments (after Luong et al., (2021) [7])

Thresholds, background concentrations, and anomalies of hydrocarbon gases in surface sediment in the southwest sub-basin of the East Vietnam Sea

As mentioned above, the hydrocarbon gas concentrations in the surface sediments obtained in the shallow-water areas of the continental shelf and slope (mainly from the Lavrentyev cruise - LV series) are much higher than those of deeper-water regions in the Southwest sub-basin EVS (mainly from the DK105 cruise - KC series). This disparity may come from the difference in the geological structures. The sampling locations during the expedition of the DK-105 cruise were spread out in the southwest sub-basin areas of EVS, while the Lavrentyev cruise operated along the 109^{o} meridian fault zone and the Northeast-Southwest fault system in the Nam Con Son basin. Obzhirov et al., (2004) [31] suggested that the fault system is the main transport channel for gases from deep structures below the seafloor.

Hence, the threshold values, background concentrations, and anomalies in the studied area were calculated for the KC series and LV series to ensure the consistency of the related geological structures. The values of 2.2 ppm and 103 ppm are the background concentration of methane distributed in the sediments, respectively, for the KC and LV series. While no anomalous value of methane was detected in the KC series, two unusually high values were detected in the samples LV88-10GC-3 (440 ppm) and LV88-07GC-2 (400 ppm) of the LV series, recovered in the Eastern part of the Nam Con Son basin (Fig. 7). Notably, previous studies have recorded high methane concentrations in the water column in this area. Shakirov et al., (2018, 2019) [4, 5] pointed out five gas geochemical regions in the EVS; one from the eastern Nam Con Son basin has the highest value of methane released into the atmosphere. In the vicinity of the Nam Con Son basin, Luong et al., (2019) [6] recorded high methane values in bottom water at a depth of 110–280 m, with the highest value of 1540 nL/L. According to Shakirov et al., (2021) [9], anomalously high methane detected in the water column up to 4,000 nL/L in 2019 could be compared with those in the oil and gas basins of the Sakhalin continental shelf.

As noted, Luong et al., (2019) [6] showed a contrast variability in the methane concentration in the bottom water of the Western part of the EVS, with low methane concentration in the deep-water areas (500–3,800 m) and higher methane concentrations in shallow-water areas of the continental shelf and

slopes (30–500 m). The data are very similar to the results of hydrocarbon gases in surface sediments in the Southwest sub-basin of the EVS. Indeed, the methane in the surface sediments in the deep-water part of this area is significantly lower than in the shallow-water areas of the continental shelf and slopes. Consequently, this study's analytical result of hydrocarbon gases implies a large-scale degassing zone along the 109^{o} meridian fault zone and the Northeast-Southwest fault system in the Nam Con Son basin.

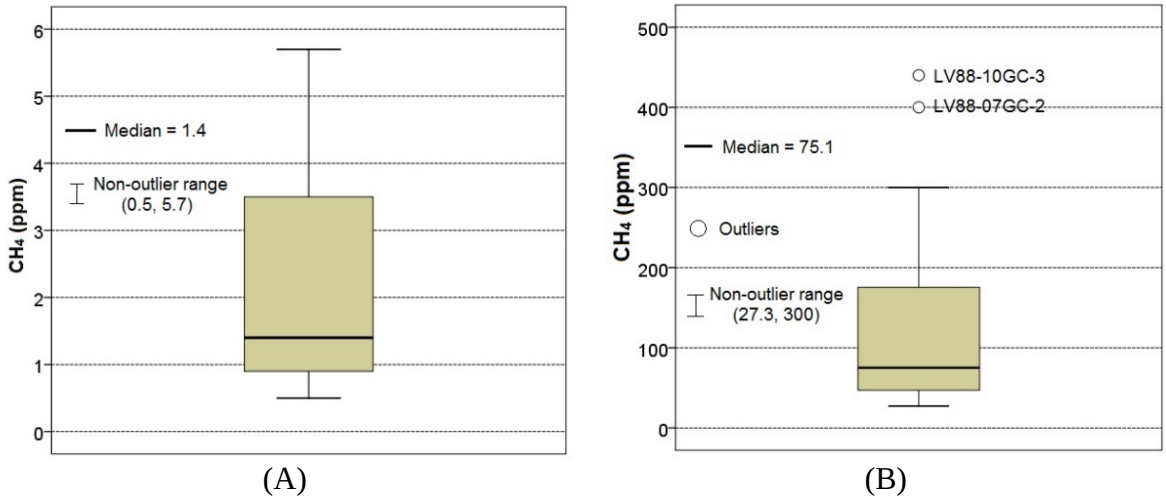

Figure 7. Boxplot showing methane concentration for the KC (A) and LV series (B), with anomalous values detected in samples LV88-10GC-3 (440 ppm) and LV88-07GC- 2 (400 ppm)

The values of 0.11 ppm and 7.45 ppm could be considered the background concentration of ethylene gas in the surface sediments of the KC and LV series, respectively. In addition, there is an ethylene anomaly in the sample KC09/19-03-1 (0.2 ppm) of the KC series, while anomalously high ethylene was found in the samples LV88-10GC-3 (70 ppm), LV88-07GC-2 (64 ppm), LV88-08GC (56 ppm), and LV88-10GC-2 (30 ppm). Noticeably, samples with ethylene anomalies in the LV series, such as LV88-10GC-3 and LV88-07GC-2, also showed anomalously high methane (Fig. 8).

Figure 8 presents the distribution of hydrocarbon concentration in the surface sediments of the LV series from South to North, starting from station LV88-01GC. The threshold values and background concentration of the gases are also shown. Thereby, the anomalies of hydrocarbon gases are displayed on the line and mainly distributed from station LV88-05GC to station LV88-10GC. These stations are located in the active area of the 109^{o} meridian fault zone, along with the Northeast-Southwest fault system. These faults play a vital role as channels carrying hydrocarbon gases from deeper parts to the surface of the sea floor.

For ethane, two anomalous values were found in sample KC09/19-02-2 (0.9 ppm) of the KC series and sample LV88-07GC-2 (124 ppm) of the LV series. The values of 0.0056 ppm and 24.2 ppm are the background concentration of ethane gas in the surface sediments of the KC and LV series, respectively. Sample LV88-07GC-2 was also the one in which methane and ethylene anomalies were found (Fig. 8).

The background concentration of propane gas in the surface sediments of the KC and LV series was 0.029 ppm and 5.92 ppm, respectively. An anomaly was found in sample KC09/19-02-2 (0.9 ppm) of the KC series. Meanwhile, three anomalies were found in the LV series in samples LV88-

09GC-2 (50 ppm), LV88-10GC-3 (24 ppm) and LV88-07GC-2 (24 ppm). Interestingly, sample LV88-10GC-3 and sample LV88-07GC-2 were also found for methane, ethylene, and ethane anomalies (Fig. 8).

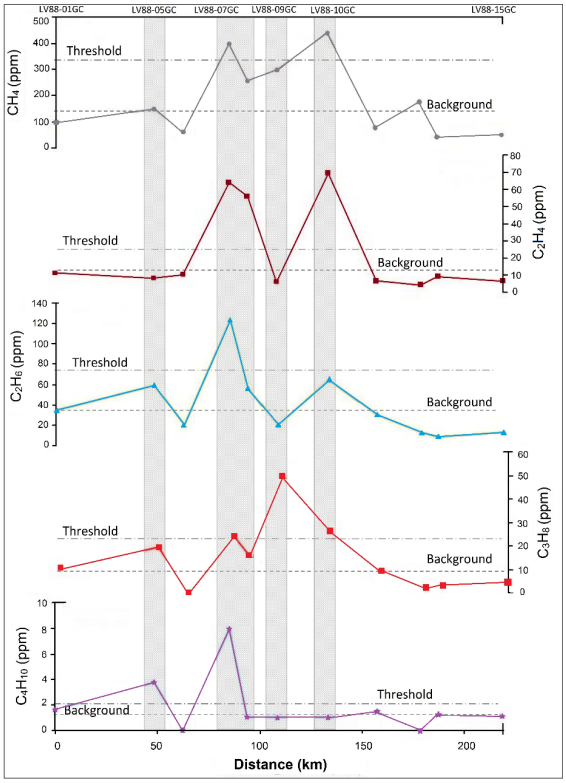

Figure 8. Distribution of highest hydrocarbon gas concentrations in the surface sediments of the LV series from South to North

Butane gas in the surface sediment of the studied area has two isoforms, including butane and i-butane. However, in the KC series, these gases were almost undetectable. In the LV series, butane and i-butane were found in 38.5% and 17.9% of the analyzed samples. The background concentration of butane gas in the surface sediments at the LV series is 0.625 ppm. There are four anomalies detected in the samples LV88-07GC-2 (8 ppm), LV88-07GC-1 (6 ppm), LV88-05GC-2 (3.78 ppm), and LV88-05GC-2 (3.77 ppm). Sample LV88-07GC-2 is also the sample where methane, ethylene, ethane, and propane anomalies were recorded.

Distribution of carbon dioxide, hydrogen, and helium in surface sediment of the Southwest sub-basin East Vietnam Sea

Carbon dioxide, hydrogen, and helium are analyzed for both R/V Akademik M.A. Lavrentyev and DK-105 samples. The concentrations of carbon dioxide, hydrogen, and helium in the surface sediment of the studied area are presented in Tables 1, 2.

Carbon dioxide concentration in surface sediments is in a wide range from 0.07% to 3.13%. Much like the case of hydrocarbon gases, carbon dioxide concentrations in surface sediments in the shallow-water continental shelf and slope areas are significantly higher than in deep-water regions (Table 1). Thus, carbon dioxide decreases considerably from the West to the East, from the shallow-water area to the deeper-water site.

The helium and hydrogen in the surface sediments were also determined for DK105 and Lavrentyev cruises. Table 2 shows that the hydrogen concentration is in a relatively wide range of 0.2–148.3 ppm (Fig. 9). Meanwhile, helium concentrations range from 0 ppm to 12.7 ppm (Fig. 10). Unlike the case of hydrocarbon gases and carbon dioxide, some locations in the deep-water area have significantly higher concentrations of hydrogen and helium than those in the shallow-water area of the continental shelf and slopes (Table 2, Figures 9, 10). Figure 9 shows some sites with the highest hydrogen concentration, including LV88-15GC (148.3 ppm), KC09/19-08 (57 ppm), and LV88-10GC (50 ppm). Generally, hydrogen gas distribution in the surface sediments in the studied area does not show the same regularity as hydrocarbon gases.

Figure 10 shows the distribution of helium concentration in surface sediment of the studied area. The highlight is the higher helium concentration at the sampling locations in the shallow-water area compared to the deep-water site of the southwest sub-basin EVS. This feature is somewhat similar to the distribution of hydrocarbon gases in surface sediment. The two positions with the highest concentrations were LV88-15GC (12.7 ppm) and LV88-01GC (8.4 ppm), distributed at the North and South poles of the LV series, respectively.

Table 2. Concentrations of helium and hydrogen in surface sediment of the Western EVS

No.	Station	Depth (m)	Interval (cm)	He (ppm)	H_2 (ppm)
1	KC09/19-02	754	20	1.8	1.3
2			100	2.9	11.8
3			200	2.1	4.6
4	KC09/19-03	1113	20	1.5	7.4
5			100	0.8	7.3
6	KC09/19-04	640	20	2.1	10.6
7			100	0.8	8.7
8	KC09/19-05	754	20	1.6	37
9			100	1.4	7.6
10	KC09/19-06	1677	50	1.4	11.8
11			100	1.2	20.5
12	KC09/19-08	1985	20	0	0.2
13			100	0.4	56.7
14	KC09/19-10	1373	20	1.1	26
15			100	0.9	7.4
16	KC09/19-20	2123	20	0.5	9.1
17			100	0.3	6.3
18	LV88-01GC	400	20	-	-
19			150	8.4	17.2
20	LV88-05GC	243	20	-	-
21			140	5.2	13.7
22	LV88-06GC	852	350	1.7	7.5
23	LV88-07GC	196	50	1.7	1.6
24			100	1.7	4.2
25	LV88-08GC	682	70	-	-
26			250	2.1	29.5
27	LV88-09GC	159	30	-	-
28			80	3.4	2.3
29	LV88-10GC	1011	40	-	-
30			200	1.5	50.4
31			300	0.8	1.5
32	LV88-11GC	267	50	3.7	23.9
33			250	1.3	4.8
34	LV88-12GC	263	20	-	-
35			80	0.9	1.8
36	LV88-14GC	256	50	0.9	1.4
37			200	0.9	4
38	LV88-15GC	236	50	2	13.1
39			200	12.7	148.3

Note: KC series from Luong et al., (2021) [7]; LV series from Shakirov et al., (2021) [32].

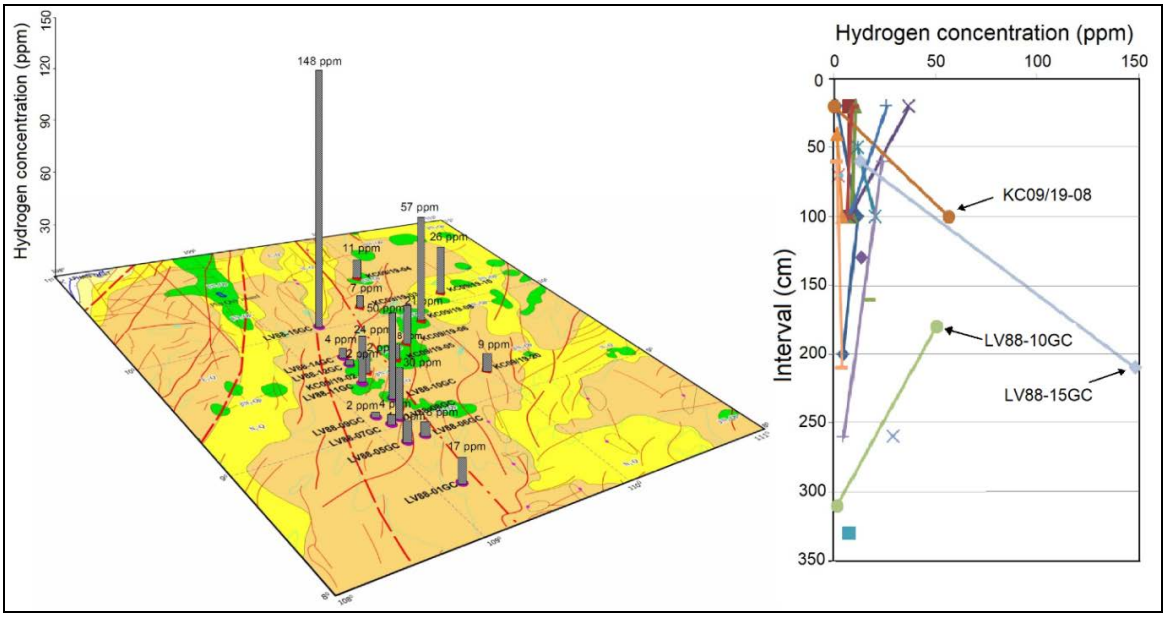

Figure 9. Distribution of hydrogen concentration in surface sediments in the Southwest sub-basin of EVS (after Luong et al., (2021) and Shakirov et al., (2021) [7, 33])

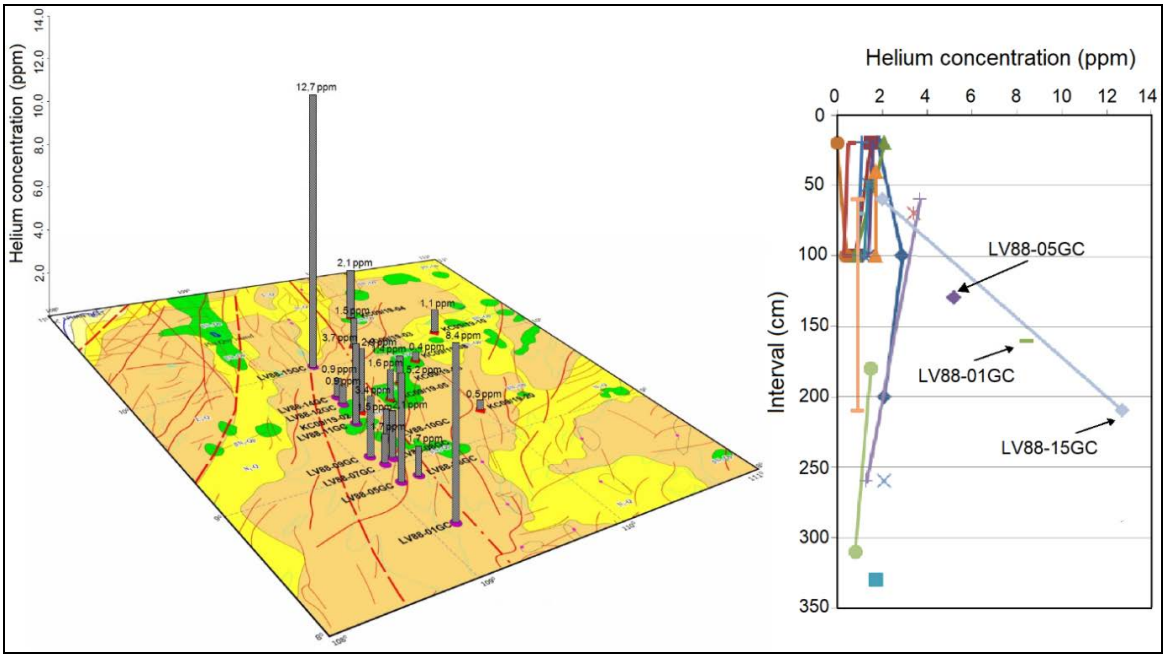

Figure 10. Distribution of helium concentration in surface sediments in the Southwest sub-basin of EVS (after Luong et al., (2021) and Shakirov et al., (2021) [7, 33])

Thresholds, background concentrations and anomalies of carbon dioxide, hydrogen, and helium in surface sediment of the Southwest sub-basin East Vietnam Sea

The background concentrations, thresholds, and anomalous values of carbon dioxide, hydrogen, and helium in the studied area are also calculated in two data series, the

LV series and the KC series, to ensure the consistency of the geological structure. Accordingly, the background data set of carbon dioxide in sediments at the KC and LV series ranges from 0.07–0.14 ppm and 0.27–3.13 ppm, respectively. The values of 0.11 ppm and 1.34 ppm could be considered the background concentration of carbon dioxide in the surface sediments of the KC and LV series, respectively. In addition, no anomalous values of carbon dioxide were detected in either series.

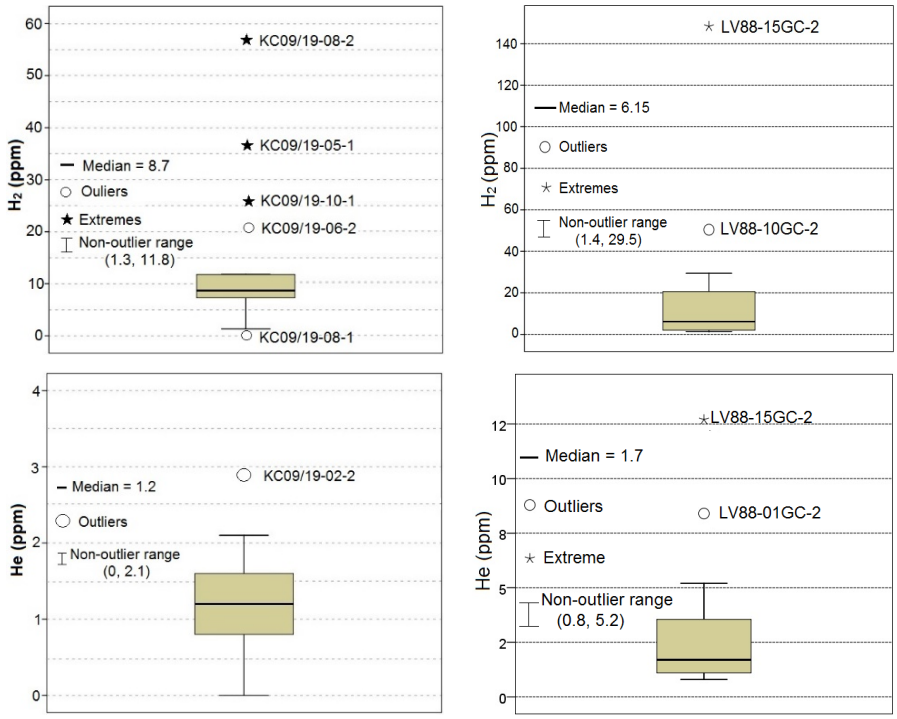

Figure 11. Boxplot showing hydrogen (top row) and helium (bottom row) concentrations in the sediments of the KC and LV series, with anomalous values detected in both series

For the KC series, four anomalous values of hydrogen in the surface sediments were detected at samples KC09/19-08-2 (56.7 ppm), KC09/19-05-1 (37 ppm), KC09/19-10-1 (26 ppm), KC09/19-06-2 (20.5 ppm) (Fig. 11). The value of 7.83 ppm could be considered the background concentration of hydrogen gas in the surface sediments of the KC series in the studied area. In addition, two hydrogen anomalies were found in the LV series at samples LV88-15GC-2 (148.3 ppm) and LV88-10GC-2 (50.4 ppm) (Fig. 11). The background concentration of hydrogen gas in the surface sediments in the LV series is 9.04 ppm.

For the LV series, two anomalously high values of helium concentration were recorded at samples LV88-15GC-2 (12.7 ppm) and LV88-01GC-2 (8.4 ppm). The analysis result showed that the value of 1.12 ppm could be considered the background concentration of helium in the surface sediments of the KC series. In addition, a positive anomaly point was found at the sample KC09/19-02-2 (2.9 ppm) (Fig. 11). Besides, the value of 1.99 ppm could be considered the background concentration of helium gas in the surface sediments of the LV series.

Origin of gases in surface sediment in the Southwest sub-basin of East Vietnam Sea

Origin of hydrocarbon gases according to hydrocarbon ratios

Bernard et al., (1976) [34] studied hydrocarbon gases in surface sediments from

the Gulf of Mexico and indicated that hydrocarbon gases are the product of two main processes: natural gases and thermogenic gases. Obzhirov et al., (2004) [31] pointed out four sources of methane gas in the seawater column of the Sea of Okhotsk, which are oil- and gas-bearing sediments, decomposition of as hydrate, atmospheric methane transfer through the sea surface, and microbial methane production. According to Yatsuk et al., (2019) [35], thermal hydrocarbon gas is a product of deep hydrocarbon metabolism, mainly affected by temperature and pressure. When comparing the geochemical characteristics of parent rock, oil, and gas in the Cuu Long and Nam Con Son sedimentary basins, Tien et al., (2008) [36] showed that the Nam Con Son basin mainly has gas potential and little potential for oil capacity. The studied area's Western part primarily belongs to the Nam Con Son basin, a vast source of hydrocarbon gases for bottom sediments and seawater through fault systems.

The ratios $C_1/(C_2+C_3)$, C_1/C_2, $C_2/C_{2:1}$, and $(C_2+C_3)/C_1$ are important ratios that have long been used in determining the origin of hydrocarbon gases [34, 35, 37–44]. The symbols C_1, C_2, $C_{2:1}$, and C_3 represent the concentrations of methane, ethane, ethylene, and propane, respectively. Hence, the hydrocarbon gas ratios were calculated to explain the origin of hydrocarbons in surface sediments in the studied area.

Bernard et al., (1976) [34] used the ratio $C_1/(C_2+C_3)$ to distinguish hydrocarbon gases of biological origin and thermal origin in active seepage zones on the seafloor in the Gulf of Mexico. Kvenvolden and Redden (1980); Kvenvolden et al., (1981), and Kvenvolden (1988) [39, 40, 41] continued to use this ratio to determine the origin of hydrocarbons in seabed sediments in the continental shelf, slope and deep basin in the Bering Sea and the South Pacific. Accordingly, when the values of this ratio are more significant than 1,000; it is a sign of hydrocarbon gas of biological origin, which is the product of the decomposition of organic matter by microorganisms. While this ratio of less than 50 indicates a thermal source, values between 50–1,000 are of mixed origin. In addition, other studies by Hachikubo et al., (2010) and Yatsuk et al., (2019) [35, 44] also used this ratio to determine the sources of hydrocarbon gas production as thermal, mixed, and biological origin, respectively.

Figure 12 shows the ratio $C_1/(C_2+C_3)$ of hydrocarbon gases in surface sediments in the Southwestern sub-basin EVS following water column depth. Samples of the KC series have a relatively wide range of $C_1/(C_2+C_3)$ ratios of 11.7–116.7, indicating that the hydrocarbon gases in the surface sediments in the shallow-water area of the continental shelf and slope have a thermal origin, while those in the deeper water area of the Southwest sub-basin EVS have mixed origin. The $C_1/(C_2+C_3)$ ratios in samples collected during the Lavrentyev cruise in the continental shelf and slope shallow-water areas, having values mostly less than 10, are almost lower than those collected from the DK105 cruise.

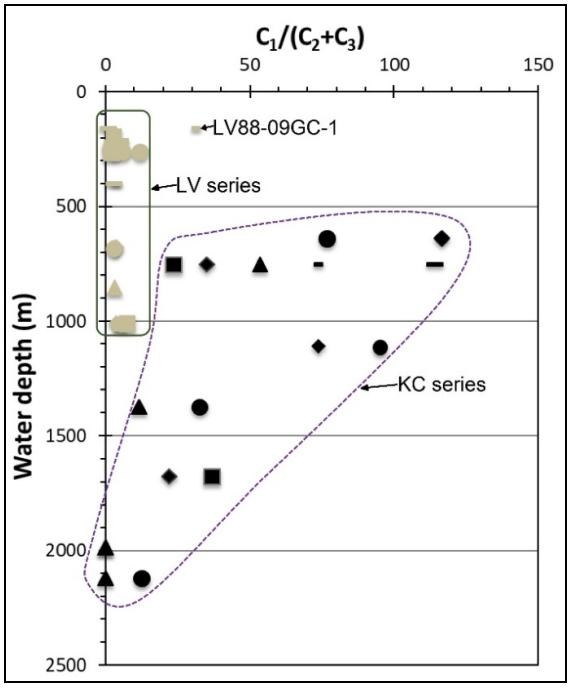

Figure 12. The $C_1/(C_2+C_3)$ ratios of methane, ethane, and propane gases of surface sediments in the Southwest sub-basin EVS

According to Pimmel and Claypool (2001) [43], the C_1/C_2 ratio is usually used to obtain quick information on the origin of hydrocarbon

gas. If this ratio is high, it indicates the process of methane formation from a biological source. On the other hand, large amounts of ethane at shallow depths are associated with thermal hydrocarbon production. The amount of ethane could be produced during the early diagenesis of organic matter and increases gradually with the burial depth, leading to a decrease in the C_1/C_2 ratio with increasing temperature. The relationship between the C_1/C_2 ratio and the sediment temperature could be used to evaluate the abnormal or normal hydrocarbon gas field. The anomalous low C_1/C_2 ratio values indicate the presence of a thermal hydrocarbon source migrated from deep below [43].

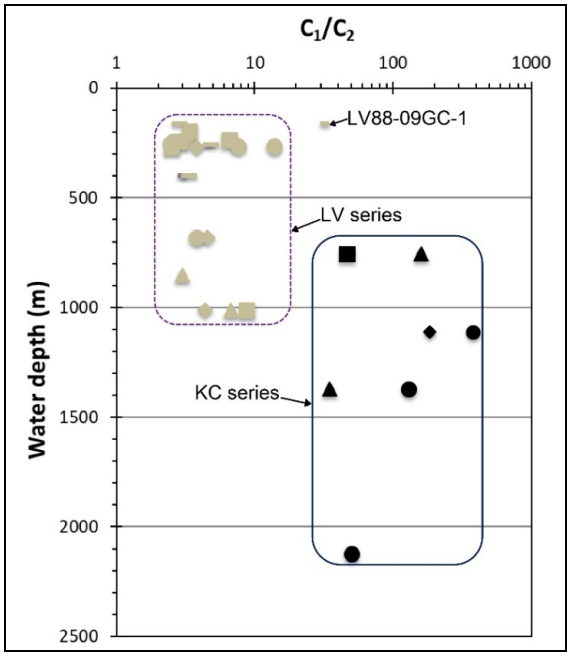

Figure 13. The C_1/C_2 ratios of ethane and ethylene gases in surface sediments in the Southwest sub-basin of EVS

Figure 13 presents the C_1/C_2 ratios following the water depth in the studied area. The striking feature is the markedly lower value of the C_1/C_2 ratio of methane and ethane in the sediments in shallow water (LV series) compared to deeper water (KC series). These values are entirely within the anomalous field as assessed by Pimmel and Claypool (2001) [43] for gases in surface sediments, suggesting that the hydrocarbon gas in the shallow water area of the continental shelf and slope has a deep thermal origin while the hydrocarbon gas in the deeper-water area is inclined to a mixed source.

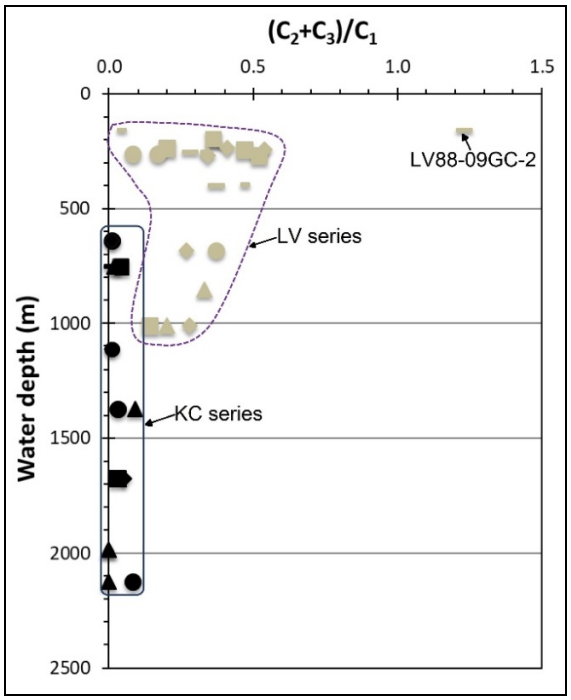

Figure 14. Ratio $(C_2+C_3)/C_1$ of methane, ethane, and propane gases in surface sediments in the Southwest sub-basin of EVS

In contrast to the $C_1/(C_2+C_3)$ ratios, the $(C_2+C_3)/C_1$ ratios can be used to distinguish the origin of hydrocarbons in sediments [35]. Accordingly, when the $(C_2+C_3)/C_1$ is < 0.1, it indicates gases originating from modern deposits; while the ratio is > 0.1, gases have a thermal origin. Figure 14 shows the ratio $(C_2+C_3)/C_1$ of hydrocarbon gases in surface sediments in the Southwest sub-basin EVS. Similar to the $C_1/(C_2+C_3)$ and C_1/C_2 ratios, there is a contrasting difference between the $(C_2+C_3)/C_1$ ratios of the KC and LV series. Accordingly, the LV series ratio is mostly higher than 0.1, while the KC series is less than 0.1. Thus, hydrocarbon gases of surface sediment samples in deep-water areas are derived from modern sediments. Meanwhile, those in shallow-water areas of continental

shelf and slope (Nam Con Son basin) have thermal oil and gas origin from deep below.

The fourth important ratio for determining the origin of hydrocarbons is $C_2/C_{2:1}$. This ratio has been used in the studies of Cline and Holmes (1977), Kvenvolden and Redden (1980), and Kvenvolden et al., (1981) [38–40]. Accordingly, because ethylene is a product of biological processes and ethane has both natural and thermal origin, a high increase in ethane relative to ethylene ($C_2/C_{2:1}$) would be an indicator of the thermal source's gas. Cline and Holmes (1977) [36] recorded an anomalously high $C_2/C_{2:1}$ ratio (6.4) in the seabed seepage in Norton Sound, Alaska, USA, and the possible source is the migration of hydrocarbon gas of thermal origin from deep-sea oil and gas.

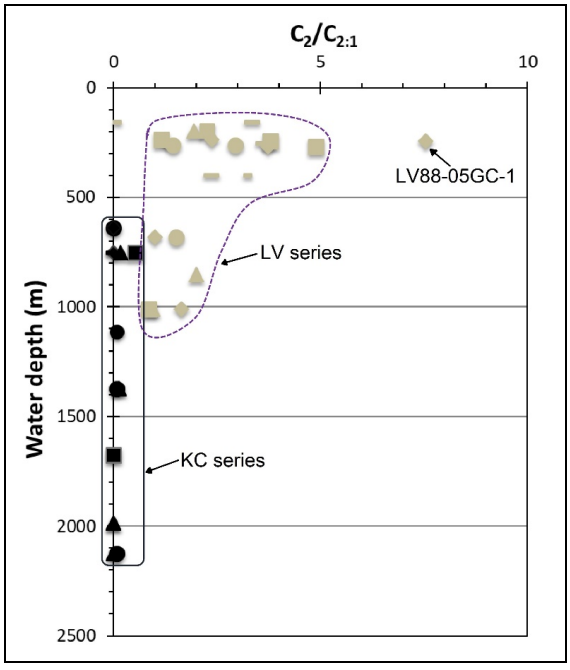

Figure 15. $C_2/C_{2:1}$ ratio of ethane and ethylene gases in surface sediments in the Southwest sub-basin of EVS

The ratio $C_2/C_{2:1}$ of ethane and ethylene gases of the surface sediments in the studied area is presented in Figure 15. The KC series ratio is less than 0.5, and that of the LV series is mostly higher than 1, especially some anomalously high-value points such as LV88-05GC-1 (7.5), LV88-11GC-1 (4.9), LV88-05GC-2 (3.8) and LV88-11GC-2 (3.7). The above gas ratios further reinforce the thermal origin of hydrocarbon gases of surface sediment samples in the shallow-water area on the continental shelf and slopes (Nam Con Son basin) and the mixed origin of those in the deeper-water area in the Southwest sub-basin EVS.

Origin of hydrocarbon gases according to carbon isotopes

The carbon isotope composition of methane has been used to explain the origin of hydrocarbon gases in marine sediments for a long time [37, 41]. In recent decades, many studies have applied carbon isotope composition to explain the origin of hydrocarbon gas in sediments in different sea regions [40–42]. Claypool and Kvenvolden (1983) [41] reported the value of carbon isotope composition of methane in sediments in many different seas worldwide. Accordingly, the value of the $\delta^{13}C$ isotope composition of methane in most samples is in the range of -90‰ to -50‰. If the methane in the near-surface sediments has a value of carbon isotope composition less than -55‰, it may originate from the processes of decomposition of organic compounds by microorganisms. Conversely, values greater than -55‰ could indicate deep-sea thermal-derived methane migrating to the seafloor surface [41].

When studying the maturation process of hydrocarbons over time and the relationship with the isotopic composition of carbon; Tien et al., (2006) [32] pointed out the change of organic material in three phases. The first phase is the biochemical gas phase in diagenesis, and $\delta^{13}C$ has a value from -90‰ to -50‰. In the middle phase, $\delta^{13}C$ value ranges from -45‰ to -25‰, while in the third phase, $\delta^{13}C$ has a value from -30‰ to -20‰.

Syrbu et al., (2021) [45] reported the values of isotope composition $\delta^{13}C$ of carbon dioxide and methane in the surface sediments in the Nam Con Son basin. Gas samples were taken from the expedition of the Lavrentyev cruise in 2019. the isotopic composition $\delta^{13}C$ of methane

in the sediments mostly has values of heavy isotope from -29.4‰ to -25.7‰, indicating the thermal origin of methane on the surface in the studied area. In addition, the $\delta^{13}C$ isotope composition of carbon dioxide in sediments ranged from -24.8‰ to -17.6‰ [45]; according to the studies of Golding et al., (2013) and Dutta et al., (2021) [46, 47], this composition belongs to the coal or petroleum production process (Fig. 16).

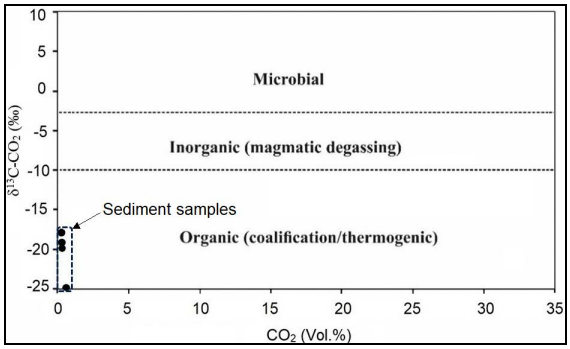

Figure 16. The $\delta^{13}C$ isotope composition of carbon dioxide in the sediments of the LV series (after Dutta et al., (2021); Syrbu et al., (2021) [45, 47])

These results strengthen the assertion about the deep thermal origin of hydrocarbon gases in the sediments in the LV series.

Relationship between the geochemical characteristics of surface sediment and surface sediment gases

Statistical analysis results for each trace element of Ag, As, Ba, Bi, Cd, Cs, Co, Cr, Cu, Mo, Ni, Pb, Sb, Sr, Zn, Sc, Y show positive anomalous values for Mo, As, Cu, and Pb (Figure 17). In particular, these anomalies are mainly concentrated in the core LV88-12GC, with very high values compared with the rest of the samples (Fig. 17). The core LV88-12GC is manifested by H_2S odor, possibly related to the hydrothermal vent field. When analyzing the total sulfide concentration of the two sediment samples at the core LV88-12GC, the value was much higher than that of the other samples, thus further reinforcing the above statement. At this site, methane concentration is high, with the highest value reaching 175.4 ppm.

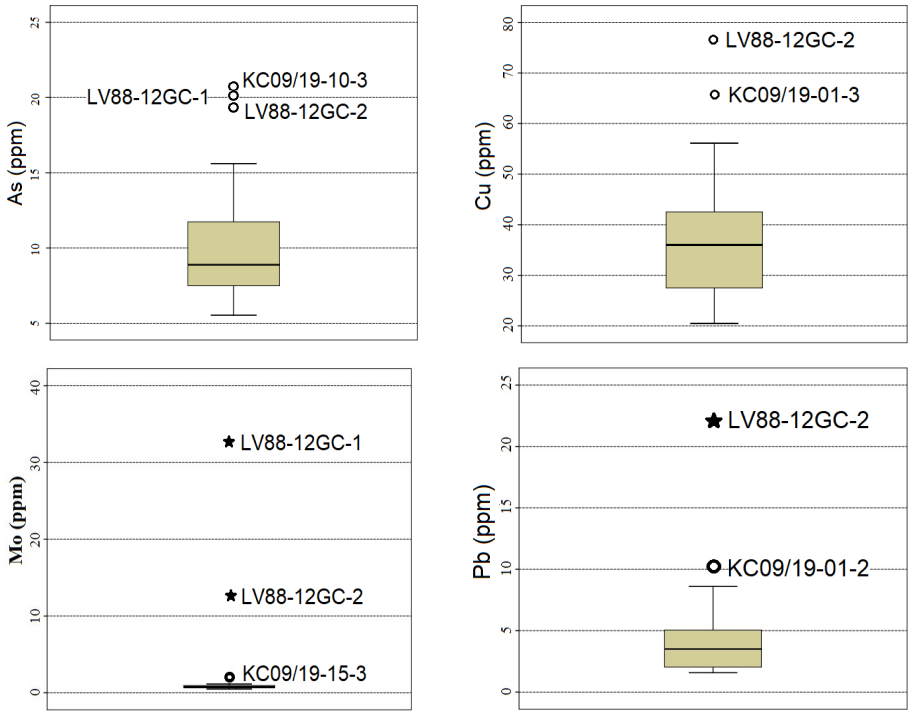

Figure 17. Anomalous values of As, Cu, Mo, and Pb at sampling locations in the studied area

Shakirov et al., (2020) [48] studied gas geochemical fields in the East Siberian Sea and showed some sampling locations with anomalies of metal concentration (e.g., Mn, V, Mo, Cu, Co, Cd, Ag) in surface sediments. This geological structure closely resembles the LV88-12GC station area, as mentioned above. Accordingly, suitable conditions for metal anomaly accumulation occur in regions with gas anomalies in active tectonic structures, whose fine-grained level is enriched with organic matter. An essential factor for accumulating these metallic elements is the biochemical processes that often occur in the region of the methane vents [48]. The geochemical fields formed in these areas could be applied as an indicator of the location of hydrocarbon accumulation for fault zone mapping and the environmental impact assessment of hydrocarbon gas anomalies.

Relationship between gases in surface sediment and fault system in the Southwest sub-basin of East Vietnam Sea

As mentioned above, the hydrocarbon gases in the KC and LV series surface sediments are of mixed and thermogenic origin, respectively. Hydrocarbon gases of the KC series have minimal concentrations and are related to modern deposits, the product of the organic matter deposition in the surface sediments. Though there are some hydrogen anomalies, this is not enough to show the influence of faults on gas composition in surface sediments of this series. Thus, the fault system's role as a gas channel from deep below in the area needs to be discussed based on the surface sediment gases in the LV series. The location is the eastern part of the Nam Con Son basin, an active area of the 109^{o} meridian fault and the Northeast-Southwest fault system (Fig. 18).

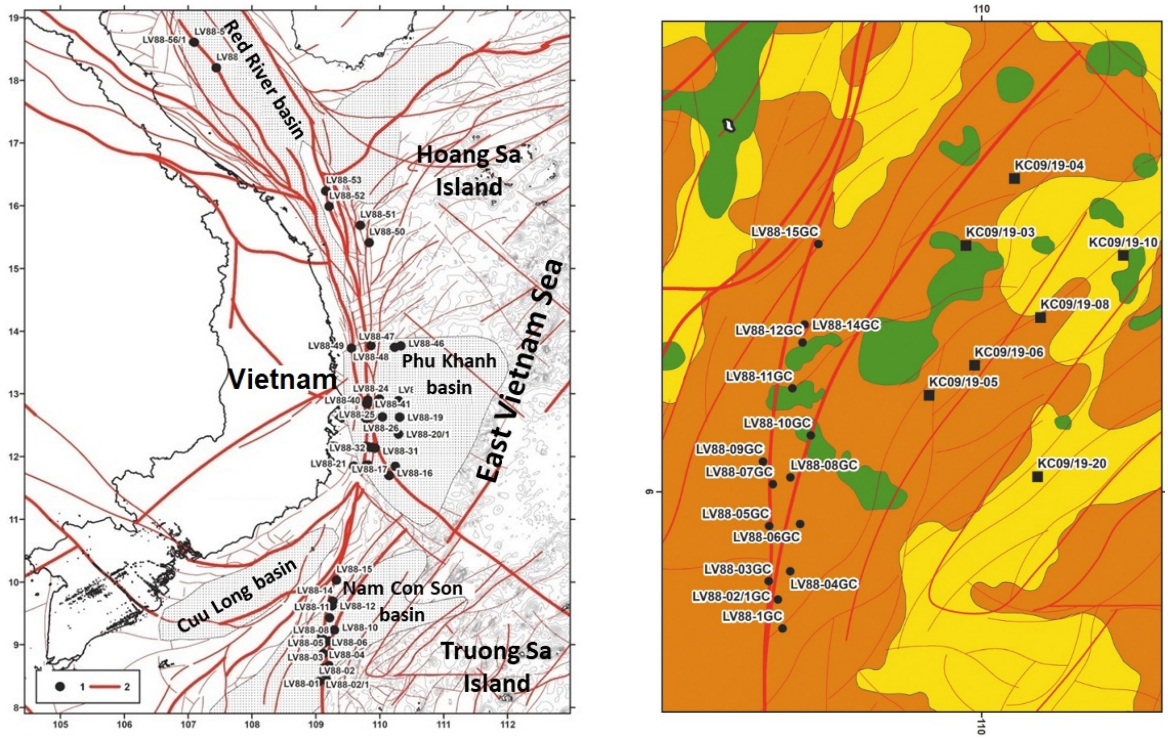

Figure 18. The sampling locations of the LV series distributed along the 109^{o} meridian fault zone and the Northeast-Southwest fault system (after Shakirov et al., (2021) [33])

The geochemical features of gases in the surface sediment samples are synthesized to evaluate the role of the fault system. The data expressed clear evidence for the vital part of

the fault systems on the gas compositions of the surface sediments along the studied area of the LV series. Tien et al., (2006) [32] showed that the heavy isotope in the gas composition reflects the ability of gas migration from the deeper part below along fault systems left by tectonic activities, forming various-scale degassing zones. Syrbu et al., (2021) [45] reported the heaviest carbon isotope compositions $\delta^{13}C$ of methane and carbon dioxide in surface sediments of this area, accompanied by anomalously high values of hydrogen and helium. Remarkably, four anomalies of hydrogen and helium concentrations were recorded at samples LV88-15GC-2 (148.3 ppm), LV88-10GC-2 (50.4 ppm) for hydrogen, and samples LV88-15GC-2 (12.7 ppm), LV88-01GC-2 (8.4 ppm) for helium. High concentrations of helium and hydrogen are usually associated with deep faults, possibly related to mantle and volcanic activity [32]. O'Nions and Oxburgh (1983) [49] showed that helium fluxes from the mantle are intensely concentrated at mid-ocean ridges but exist elsewhere in oceanic basins associated with intra-plate and marginal igneous activities. Shakirov et al., (2016) [50] studied the distribution of helium and hydrogen gases in sediments and seawater on the Sakhalin slope, the Sea of Okhotsk, and reported helium and hydrogen anomalies up to 60 ppm and 120 ppm, respectively. These anomalies were found in hydrate-bearing sediments from hydrocarbon fluid flows in fault zones [50]. Therefore, helium anomalies in surface sediments and bottom waters often identify deep faults. They are recorded even when the fault is covered by a thick layer of sediment [50]. In addition, hydrogen gas is usually associated with volcanic activity, hydrothermal vent systems, and deep faults [50].

The evidence above further proves that the gases in the Eastern part of the Nam Con Son basin (LV series) sediments have a deep thermal origin and they are closely associated with fault systems.

Comparative features of the geochemical gas field in surface sediment of the Southwest sub-basin of East Vietnam Sea and other regions of West East Vietnam Sea

Comparative features of the geochemical gas field in surface sediment of the Southwest sub-basin of East Vietnam Sea and those of Phu Khanh basin and Red river basin

The mean and maximum values of the gases in surface sediments of the southwest sub-basin EVS (LV series - Nam Con Son basin), Phu Khanh basin, and Red river basin were compared. Based on statistical methods, the background concentrations of methane gas in the surface sediments of the Nam Con Son basin, Phu Khanh basin, and Red river basin are 103 ppm, 34 ppm, and 26 ppm, respectively. Except for carbon dioxide, all hydrocarbon gas concentrations follow the decreasing trend from south to north, respectively, from the Nam Con Son basin to the Phu Khanh basin and, finally, the Red river basin. This decreasing trend reinforces the presence of a large-scale degassing zone in the studied area of the Nam Con Son basin. Thus, we constructed a diagram of methane distribution in the Western EVS surface sediments based on the methane concentration of the three basins mentioned above, (Fig. 19).

The distribution of methane in Western EVS surface sediments is consistent with methane in the seawater column of the surface and bottom layers of the West EVS according to the Lavrentyev cruise in 2019 (Fig. 20, [51]). In which the concentration of methane in the bottom water layer in the Nam Con Son basin has the highest value compared to that of the Phu Khanh basin and the Red river basin, with anomalous values up to 3,475 nL/L (station LV88-06GC); 1,404 nL/L (station LV88-08GC) and 1,505 nL/L (station LV88-10GC). This result shows an apparent similarity with the value of methane in the surface sediments, in which the 109^{o} meridian fault system in the studied area plays a critical role in the movement of gases in the sediment into the water column [52].

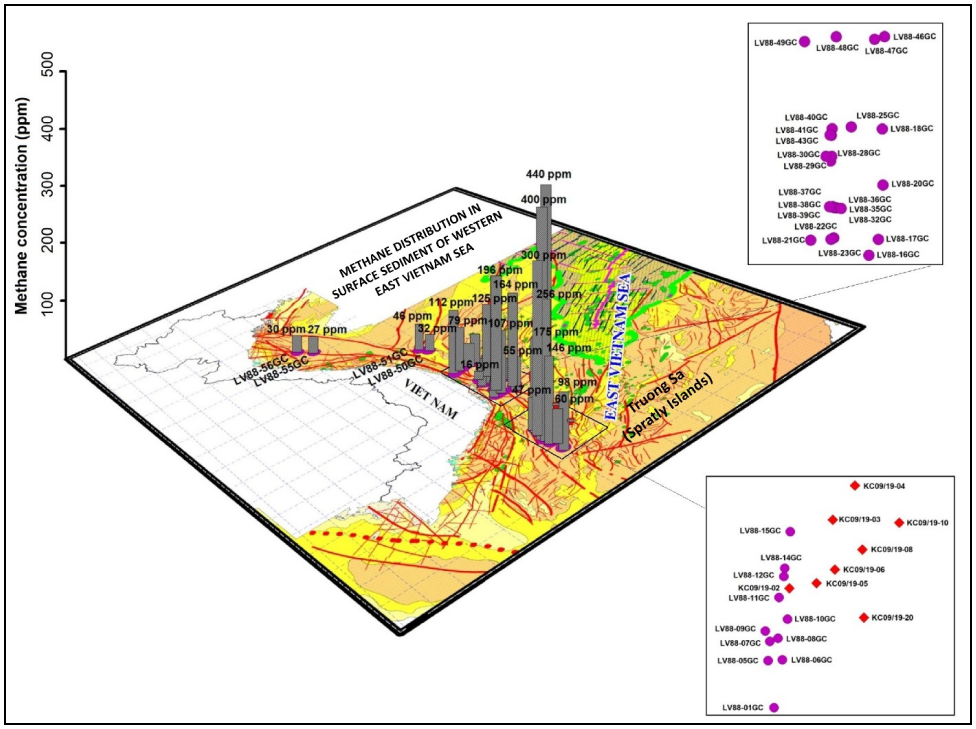

Figure 19. Scheme of methane distribution in surface sediments in the Southwest sub-basin of EVS (Nam Con Son basin), Phu Khanh basin, and Red river basin. After Geological map, geological resources of Vietnam and adjacent sea regions, scale 1:1,000,000) [29]

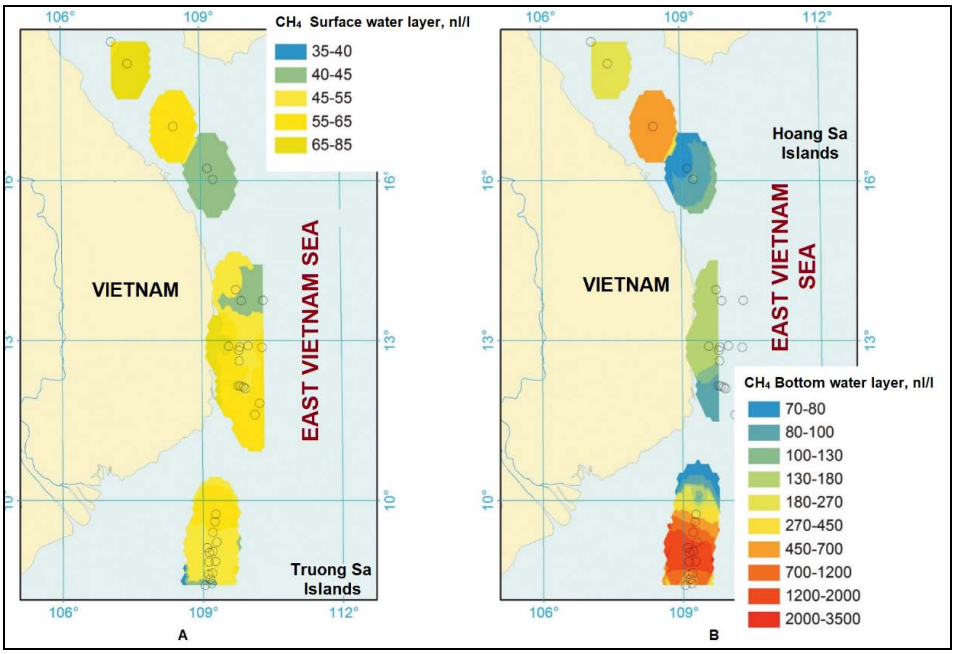

Figure 20. Distribution of methane in the seawater column of the surface water layer (A) and bottom water layer (B) in Western EVS according to the Lavrentyev cruise in November 2019 (after Telegin et al., (2021) [51])

Comparative features of the geochemical gas field in surface sediment of the Southwest sub-basin of East Vietnam Sea and those of the Gulf of Tonkin

Previous studies of gas geochemical fields in the Gulf of Tonkin reported the average concentrations of hydrocarbons, helium, and hydrogen [52, 53]. Accordingly, the average concentrations for methane, ethylene, ethane, propane, and butane gas are 3.98 ppm, 1.12 ppm, 0.18 ppm, 0.1 ppm, and 0.38 ppm, respectively. These values are often lower when compared with hydrocarbons in the Southwest sub-basin EVS surface sediments. Meanwhile, the average hydrogen gas concentration in the Southwest sub-basin EVS sediments is slightly higher than in the Gulf of Tonkin. In contrast, the helium concentration in the studied area was significantly lower than in the Gulf of Tonkin. Duong Quoc Hung et al., (2019) [54] studied the gas geochemical field of the estuary area in the northwest Gulf of Tonkin and reported the background concentration of methane is up to 4 ppm. This value is much lower than that of the Southwest sub-basin EVS.

CONCLUSION

In the southwest sub-basin of EVS, the methane concentrations in surface sediments vary widely, from 0.5 ppm to 440 ppm. This contrast variability coincides with the distribution of methane concentration in the bottom water layer. Methane was detected in all samples showing higher concentrations in the shallow-water continental shelf and slope areas than in the deeper-water areas. Other heavier hydrocarbon gases, including ethane, ethylene, propane, and butane, were also determined and expressed similar distribution in concentration with methane.

The presence of a large-scale degassing zone of hydrocarbon gases was proposed. The value of thresholds, anomalies, and background concentrations of gases in surface sediment of the southwest sub-basin EVS were calculated at the LV and KC series to ensure the similarity in geological structure. The values of 2.2 ppm and 103 ppm are the methane background concentrations distributed in the KC and LV series sediments, respectively. In addition, LV samples LV88-10GC-3 (440 ppm) and LV88-07GC-2 (400 ppm) in the eastern part of the Nam Con Son basin contained anomalous methane values. The background concentrations of carbon dioxide, hydrogen, and helium in the surface sediments or the KC and LV series were also calculated, where high hydrogen and helium were also detected in both series.

The $C_1/(C_2+C_3)$, C_1/C_2, $C_2/C_{2:1}$, and $(C_2+C_3)/C_1$ ratios of hydrocarbon gases were utilized to determine the origin of hydrocarbon gases in the Southwest sub-basin EVS. The results indicate that hydrocarbon gases in the surface sediment of the shallow-water area of the continental shelf and slope (mainly in the LV series) have a thermal origin. In contrast, in the deeper-water area (the KC series), the hydrocarbon gases have mixed origins (biological and thermal origins).

A hydrothermal vent occurred at core LV88-12GC, where positive anomalous values of elements Mo, As, Cu, and Pb were discovered. The isotope composition values have reinforced the thermal origin of hydrocarbon gases in shallow-water area $\delta^{13}C$ of carbon dioxide and methane in the surface sediments of the Nam Con Son basin. Accordingly, the isotope composition values $\delta^{13}C$ of carbon dioxide and methane in the surface sediment are mostly in ranges of -24.8‰ to -17.6‰ and -29.4‰ to -25.7‰, respectively. These values of the $\delta^{13}C$ isotope composition were produced under extreme temperature and pressure conditions, with a formation depth of at least 2 km.

The synthesized gas geochemical evidence has emphasized the deep thermal origin of the gases in the surface sediments at the LV series of the studied area. The 109^o meridian fault zone and the Northeast-Southwest fault system are vital as these gases' main channels.

The results of the comparison of methane in the sediments in the Nam Con Son basin, Phu Khanh basin, and Red river basin show that the methane background concentration decreases

gradually from South to North, with values of 103 ppm, 34 ppm, and 26 ppm for the three basins. In addition, the average values of hydrocarbon gas concentrations in the surface sediments of the studied area are much higher than those of the Gulf of Tonkin.

Acknowledgments: This study is supported by the Vietnam National project coded KC09.31/16–20, the joint project "First joint expedition on marine geophysics-geology-oceanography between VAST and FEB RAS by R/V "Akademik M.A. Lavrentyev" in the East Vietnam Sea" coded QTRU.02.05/19–20 and the Vietnam Academy of Science and Technology's project coded VAST05.03/20–21. The captain, colleagues, and crew members of the Research Vessel "Akademik M.A. Lavrentyev" cruise and the DK105 cruise in the East Vietnam Sea are also thanked for sampling and technical supports. The authors also thank the anonymous reviewer for helpful and constructive comments.

REFERENCES

[1] Li, C. F., Lin, J., and Kulhanek, D. K. the Expedition 349 Scientists, 2015. South China Sea tectonics. *Proceedings of the International Ocean Discovery Program (IODP). 2015.3. 30, 349: 1, 300*.

[2] Tseng, H. C., Chen, C. T. A., Borges, A. V., DelValls, T. A., and Chang, Y. C., 2017. Methane in the South China Sea and the Western Philippine Sea. *Continental Shelf Research, 135*, 23–34. https://doi.org/10.1016/j.csr.2017.01.005

[3] Zhang, M., Lu, H., Guan, H., Liu, L., Wu, D., and Wu, N., 2018. Methane seepage intensities traced by sulfur isotopes of pyrite and gypsum in sediment from the Shenhu area, South China Sea. *Acta Oceanologica Sinica, 37*(7), 20–27. https://doi.org/10.1007/s13131-018-1241-1

[4] Shakirov, R. B., Lan, N. H., Yatsuk, A., Mishukova, G., and Shakirova, M., 2018. Methane flux into the atmosphere in the Bien Dong (East Sea of Vietnam). *Vietnam Journal of Marine Science and Technology*, 18(3), 250–255. doi: 10.15625/1859-3097/12969

[5] Shakirov, R. B., Yatsuk, A. V., Mishukova, G. I., Obzhirov, A. I., Yugai, I. G., Cuong, D. H., Lan, N. H., Legkodimov, A. A., and Shakirova, M. V., 2019. Methane flux into the atmosphere in the South China Sea. In *Doklady Earth Sciences* (Vol. 486, No. 1, pp. 533–536). *Pleiades Publishing*. https://doi.org/10.1134/S1028334X19050064

[6] Luong, L. D., Shakirov, R. B., Hoang, N., Shinjo, R., Obzhirov, A., Syrbu, N., and Shakirova, M., 2019. Features in REE and methane anomalies distribution in the East China Sea water column: a comparison with the South China Sea. *Water Resources*, *46*(5), 807–816. doi: 10.1134/S0097807819050142

[7] Luong, L. D., Obzhirov, A. I., Hoang, N., Shakirov, R. B., Anh, L. D., Syrbu, N. S., Tuan, D. M., Tao, N. V., Huong, T. T., Cuong, D. H., Kholmogorov, A. O., Binh, P. V., Mishukova, O. V., and Eskova, A. I., 2021. Distribution of Gases in Bottom Sediments of the Southwestern sub-basin South China Sea (Bien Dong). *Russian Journal of Pacific Geology*, *15*(2), 144–154. doi:10.1134/S1819714021020044

[8] Shakirov, R. B., Obzhirov, A., Shakirova, M., Jin, Y. K., and Trung, N. N., 2017. Concept of Eastern Asia gas hydrate belt. In *Tottori International Forum on Methane Hydrate* (pp. 94–95).

[9] Shakirov, R. B., Cuong, D. H., Obzhirov, A. I., Valitov, M. G., Lee, N. S., Legkodimov, A. A., Kalgin, V. Yu., Yeskova, A. I., Proshkina, Z. N., Telegin, Yu. A., Storozhenko, A. V., Ivanov, M. V., Pletnev, S. P., Sedin, V. T., Bulanov, A. V., Shvalov, D. A., Lipinskaya, N. A., Bovsun, M. A., Makseev, D. S., Thanh, N. T., Anh, L. D., and Luong, L. D., 2021. Integrated Geological–Geophysical and Oceanographic Research in the South China Sea: Cruise 88 of the R/V "Akademik MA Lavrentyev". *Oceanology*, *61*(1), 147–149. doi: 10.1134/S0001437021010173

[10] Taylor, B., and Hayes, D. E., 1980. The tectonic evolution of the South China Basin. *Washington DC American Geophysical Union Geophysical Monograph Series*, *23*, 89–104. doi: 10.1029/GM023p0089

[11] Taylor, B., and Hayes, D. E., 1983. Origin and history of the South China Sea basin. *Washington DC American Geophysical Union Geophysical Monograph Series*, *27*, 23–56. doi: 10.1029/GM027p0023

[12] Briais, A., Patriat, P., and Tapponnier, P., 1993. Updated interpretation of magnetic anomalies and seafloor spreading stages in the South China Sea: Implications for the Tertiary tectonics of Southeast Asia. *Journal of Geophysical Research: Solid Earth*, *98*(B4), 6299–6328. https://doi.org/10.1029/92JB02280

[13] PetroVietnam, 2005. Geology and oil and gas resources of Vietnam. 526 p.

[14] Li, L., and Clift, P. D., 2013. The sedimentary, magmatic and tectonic evolution of the southwestern South China Sea revealed by seismic stratigraphic analysis. *Marine Geophysical Research*, *34*(3), 341–365. https://doi.org/10.1007/s11001-013-9171-y

[15] Ding, W., Li, J., Clift, P. D., and Expedition, I. O. D. P., 2016. Spreading dynamics and sedimentary process of the Southwest Sub-basin, South China Sea: constraints from multi-channel seismic data and IODP Expedition 349. *Journal of Asian Earth Sciences*, *115*, 97–113. doi: 10.1016/j.jseaes.2015.09.013

[16] Van Phach, P., Van Tri, T., Trung, N. N., and Anh, L. D., 2018. The Geological Structure of the Southwestern end of the East Sea. *Proceeding of the 15th regional congress on Geology, Mineral and Energy resources of Southeast Asia (GEOSEA XV)*, pp. 238–241.

[17] Phuong, N. H., and Truyen, P. T., 2015. Probabilistic seismic hazard maps of Vietnam and the East Vietnam Sea. *Vietnam Journal of Marine Science and Technology*, *15*(1), 77–90. https://doi.org/10.15625/1859-3097/6083

[18] Liu, Z., Zhao, Y., Colin, C., Stattegger, K., Wiesner, M. G., Huh, C. A., Zhang, Y., Li, X., Sompongchaiyakul, P., You, C.-F., Huang, C.-Y., Liu, J. T., Siringan, F. P., Le, K. P., Sathiamurthy, E., Hantoro, W. S., Liu, J., Tuo, S., Zhao, S., Zhou, S., He, Z., Wang, Y., Bunsomboonsakul, S., and Li, Y., 2016. Source-to-sink transport processes of fluvial sediments in the South China Sea. *Earth-Science Reviews*, *153*, 238–273. doi: 10.1016/j.earscirev.2015.08.005

[19] Milliman, J. D., and Meade, R. H., 1983. World-wide delivery of river sediment to the oceans. *The Journal of Geology*, *91*(1), 1–21. doi: 10.1086/628741

[20] Schimanski, A., and Stattegger, K., 2005. Deglacial and Holocene evolution of the Vietnam shelf: stratigraphy, sediments and sea-level change. *Marine Geology*, *214*(4), 365–387. https://doi.org/10.1016/j.margeo.2004.11.001

[21] Wang, P., and Li, Q. (Eds.), 2009. The South China Sea: Paleoceanography and Sedimentology (Vol. 13). *Springer Science & Business Media*. 512 p.

[22] Shinjo, R., Shakirov, R. B., and Obzhirov, A., 2021. Chemical, mineralogical, and physicochemical features of surface saline muds from Southwestern sub-basin of the East Vietnam Sea: Implication for new peloids. *Vietnam Journal of Earth Sciences*, *43*(4), 496–508. https://doi.org/10.15625/2615-9783/16561

[23] Nguyen, H., Shinjo, R., Tran, T. H., Le, D. L., and Le, D. A., 2021. Mantle geodynamics and source domain of the East Vietnam Sea opening-induced volcanism in Vietnam and neighboring regions. *Vietnam Journal of Marine Science and Technology*, *21*(4), 393–417. doi: 10.15625/1859-3097/16856

[24] Reimann, C., Filzmoser, P., and Garrett, R. G., 2005. Background and threshold: critical comparison of methods of determination. *Science of The Total Environment*, *346*(1–3), 1–16. doi: 10.1016/j.scitotenv.2004.11.023

[25] Folk, R. L., 1974. Petrology of sedimentary rocks. *Hemphill Publishing Company, Austin, Texas 78703*.

[26] Anders, E., and Grevesse, N., 1989. Abundances of the elements: Meteoritic and solar. *Geochimica et Cosmochimica acta*, *53*(1), 197–214. https://doi.org/10.1016/0016-7037(89)90286-X

[27] McLennan, S. M., Hemming, S., McDaniel, D. K., and Hanson, G. N., 1993. Geochemical approaches to sedimentation, provenance, and tectonics. *Special Papers-Geological Society of America*, *284*, 21–40.

[28] Taylor, S. R., and McLennan, S. M., 1997. The origin and evolution of the Earth's continental crust. *AGSO Journal of Australian Geology and Geophysics*, *17*, 55–62.

[29] Center for Geological Information, Archives and Journals, General Department of Geology and Minerals of Vietnam, Ministry of Natural Resources and Environment, 2010. Geological map, geological resources of Vietnam and adjacent sea regions, scale 1:1.000.000.

[30] Nghi, T., 2010. Sedimentology in marine geology and petroleum. *Vietnam National University Press, Hanoi*, 326 p.

[31] Obzhirov, A., Shakirov, R., Salyuk, A., Suess, E., Biebow, N., and Salomatin, A., 2004. Relations between methane venting, geological structure and seismo-tectonics in the Okhotsk Sea. *Geo-marine letters*, *24*(3), 135–139. https://doi.org/10.1007/s00367-004-0175-0

[32] Tien, H.D, 2006. Petroleum geology and methods of prospecting, exploration, monitoring oil and gas field. *Vietnam National University Ho Chi Minh City Press*, 536 p.

[33] Shakirov, R. B., Valitov, M. G. Lee, N. S., Hoang, N., and Phach, P. V., 2021. Monograph: Geologic-geophysical and oceanographic research of the western South China sea and adjacent continent (on results of the RV “Akademik M.A. Lavrentyev” cruise 88 and coastal surveys 2010–2020). *Moscow, GEOS*, 412 p.

[34] Bernard, B. B., Brooks, J. M., and Sackett, W. M., 1976. Natural gas seepage in the Gulf of Mexico. *Earth and Planetary Science Letters*, *31*(1), 48–54. doi: 10.1016/0012-821X(76)90095-9

[35] Yatsuk, A., Shakirov, R., Gresov, A., and Obzhirov, A., 2020. Hydrocarbon gases in seafloor sediments of the TATAR strait, the northern sea of Japan. *Geo-Marine Letters*, *40*(4), 481–490. https://doi.org/10.1007/s00367-019-00628-5

[36] Tien, H. D., Chat, H. C., Dung, N. N., and Anh, N. N., 2008. Comparison of geochemical characteristics of parent rock and petroleum in two sedimentary basins Cuu Long and Nam Con Son. *Science & Technology Development*, *11*(11), 106–118.

[37] Claypool, G. E., Presley, B. J., and Kaplan, I. R., 1973. Gas analyses in sediment samples from Legs 10, 11, 13, 14, 15, 18, and 19. In *Creager, J. S., Scholl, D. W, et al., Init. Repts. DSDP, 19: Washington (U.S. Govt. Printing Office)*, 879–884.

[38] Cline, J. D., and Holmes, M. L., 1977. Submarine seepage of natural gas in Norton Sound, Alaska. *Science*, *198*(4322), 1149–1153. doi: 10.1126/science.198.4322.1

[39] Kvenvolden, K. A., and Redden, G. D., 1980. Hydrocarbon gas in sediment from the shelf, slope, and basin of the Bering Sea. *Geochimica et Cosmochimica Acta*, *44*(8), 1145–1150. https://doi.org/10.1016/0016-7037(80)90068-X

[40] Kvenvolden, K. A., Vogel, T. M., and Gardner, J. V., 1981. Geochemical prospecting for hydrocarbons in the outer continental shelf, southern Bering Sea, Alaska. *Journal of Geochemical Exploration*, *14*, 209–219. https://doi.org/10.1016/0375-6742(81)90113-8

[41] Claypool, G. E., and Kvenvolden, K. A., 1983. Methane and other hydrocarbon gases in marine sediment. *Annual Review of Earth and Planetary Sciences*, *11*, 299–327. https://doi.org/10.1146/annurev.ea.11.050183.001503

[42] Kvenvolden, K. A., 1988. Hydrocarbon gas in sediment of the southern Pacific Ocean. *Geo-marine letters*, *8*(3), 179–187. https://doi.org/10.1007/BF02326095

[43] Pimmel, A., and Claypool, G., 2001. Introduction to shipboard organic geochemistry on the JOIDES Resolution. ODP Technical Note, 30, 29 pages. Address: http://www-odp.tamu.edu/publications/tnotes/tn30/index.htm.

[44] Hachikubo, A., Krylov, A., Sakagami, H., Minami, H., Nunokawa, Y., Shoji, H., Matveeva, T., Jin, Y. K., and Obzhirov, A., 2010. Isotopic composition of gas hydrates in subsurface sediments from offshore Sakhalin Island, Sea of Okhotsk. *Geo-Marine Letters*, *30*(3), 313–319. https://doi.org/10.1007/s00367-009-0178-y

[45] Syrbu, N. S., Cuong, D. H., Iakimov, T. S., Kholmogorov, A. O., Telegin, Y. A., and Tsunogai, U., 2021. Geological features for the formation of gas-geochemical fields, including helium and hydrogen, in the water and sediments at the Vietnamese part of the South-China Sea. *Georesursy = Georesources*, *23*(3), 132–142. doi: 10.18599/grs.2021.1.16

[46] Golding, S. D., Boreham, C. J., and Esterle, J. S., 2013. Stable isotope geochemistry of coal bed and shale gas and related production waters: A review. *International Journal of Coal Geology*, *120*, 24–40. https://doi.org/10.1016/j.coal.2013.09.001

[47] Dutta, S., Ghosh, S., and Varma, A. K., 2021. Methanogenesis in the Eocene Tharad lignite deposits of Sanchor Sub-Basin, Gujarat, India: Insights from gas molecular ratio and stable carbon isotopic compositions. *Journal of Natural Gas Science and Engineering*, *91*, 103970. doi: 10.1016/j.jngse.2021.103970

[48] Shakirov, R. B., Sorochinskaja, A. V., Syrbu, N. S., Tsunogai, U., and Yen, T. H., 2020. Gas-geochemical studies of gas fields and increased metal concentrations in the East Siberian Sea. *Vietnam Journal of Earth Sciences*, *42*(4), 395–410. doi: 10.15625/0866-7187/42/4/15492

[49] O'nions, R. K., and Oxburgh, E. R., 1983. Heat and helium in the Earth. *Nature*, *306*(5942), 429–431. https://doi.org/10.1038/306429a0

[50] Shakirov, R. B., Syrbu, N. S., and Obzhirov, A. I., 2016. Distribution of helium and hydrogen in sediments and water on the Sakhalin slope. *Lithology and mineral resources*, *51*(1), 61–73. doi: 10.1134/S0024490216010065

[51] Telegin, Y. A., Obzhirov, A. I., and Shakirov, R. B., 2021. Gasgeochemical fields in the water column. Monograph: Geologic-geophysical and oceanographic research of the western South China sea and adjacent continent (on results of the RV "Akademik M.A. Lavrentyev" cruise 88 and coastal surveys 2010–2020). *Moscow*, *GEOS*, 412 p.

[52] Akulichev, V. A., Obzhirov, A. I., Shakirov, R. B., Van Phach, P., Trung, N. N., Hung, D. Q., Mal'tseva, E. V., Syrbu, N. S., Polonik, N. S., and Polonik, N. S., 2015. Anomalies of natural gases in the Gulf of Tonkin (South China Sea). In *Doklady Earth Sciences* (Vol. 461, No. 1, pp. 203–208). *Springer*. https://doi.org/10.1134/S1028334X15030010

[53] Le, D. A., Trung, N. N., Phach, P. V., Hung, D. Q., Diep, N. V., Nam, B. V., Shakirov, R. B., Obzhirov, A. I., Ugai, I. G., Mal'tseva, E. V., Telegin, Yu. A., and Syrbu, N. S., 2014. Characteristics of helium, methane and hydrogen distribution and their relationship with fault systems in the north of the Gulf of Tonkin. *Vietnam Journal of Marine Science and Technology*, *14*(4A), 78–89.

[54] Hung, D. Q., Shakirov, R., Iugai, I., Van Diep, N., Dong, M. D., Van Nam, B., and Telegin, Y., 2019. A study on the relationship between gas-geochemical field and tectonic fault activities in the rivermouth area of northwestern Gulf of Tonkin. *Vietnam Journal of Marine Science and Technology*, *19*(2), 191–198. https://doi.org/10.15625/1859-3097/14036